

Chert concretions and bedded cherts from the southeastern Franconian Alb, Bayerwald and Kraków-Częstochowa Upland as potential raw materials for artifact manufacturing in the Paleolithic, Mesolithic and Neolithic – a comparative petrographic study

Alicja KOCHMAN¹, * and Jacek MATYSZKIEWICZ¹

¹ AGH University of Krakow, Faculty of Geology, Geophysics and Environmental Protection, al. Mickiewicza 30, 30-059 Kraków, Poland; ORCID: 0000-0002-4003-6513 [A.K.], 0000-0002-1812-9967 [J.M.]



Kochman, A., Matyszkiewicz, J., 2025. Chert concretions and bedded cherts from the southeastern Franconian Alb, Bayerwald and Kraków-Częstochowa Upland as potential raw materials for artifact manufacturing in the Paleolithic, Mesolithic and Neolithic – a comparative petrographic study. *Geological Quarterly*, **69**, 12; <https://doi.org/10.7306/gq.1785>

The Upper Jurassic carbonate deposits of microbial-sponge megafacies, which host chert concretions and bedded cherts, were deposited along the northern margin of the Tethyan Ocean. Exposures of these rocks extend from Portugal to the Caucasus Mts. Well-known localities include those in southeastern Germany and southern Poland, where these strata are similar in lithology. Petrographic studies on chert concretions and bedded cherts from Upper Jurassic successions exposed in the southeastern part of the Franconian Alb and in the Bayerwald have shown that silicification was a late-diagenetic, multi-stage process and that the silica presumably originated from hydrothermal solutions. The chert concretions of the Bayerwald show considerable similarity to lithologies known from the Kraków-Częstochowa Upland. In both regions, these mostly represent silicified microbial-sponge biostromes. By contrast, the chert concretions of the Franconian Alb, where younger parts of the Upper Jurassic succession are preserved, differ significantly from the concretions encountered in both the Bayerwald and the Kraków-Częstochowa Upland. The bedded cherts of the Franconian Alb are partly silicified tempestite sequences whereas those of the Kraków-Częstochowa Upland represent silicified calciturbidites. However, some fine-grained portions of these successions show macroscopic resemblance, despite their differences in development. In prehistoric times, these regions in Poland and Germany were sources of siliceous raw-materials, which might have been exported towards Bohemia, as suggested by artifacts that are believed to have originated from Poland or Germany. However, comparative studies indicate that macroscopic diagnostic features determining the origin of artifacts manufactured from either the chert concretions or the bedded cherts are of doubtful value. In particular, the “chocolate flint” distinguished by archaeologists, the origin of which is suggested to be limited exclusively to the northeastern margin of the Holy Cross Mts. or to the central part of the Kraków-Częstochowa Upland, may also represent parts of chert concretions collected in the Franconian Alb. Distinction of this variety in artifact inventories based upon individual specimens may be erroneous.

Key words: chert concretions, bedded cherts, siliceous artifacts, Franconian Alb, Bayerwald, Kraków-Częstochowa Upland.

INTRODUCTION

Archaeological literature on Paleolithic, Mesolithic and Neolithic materials in the eastern part of Central Europe describes various siliceous raw materials including the “Jurassic flint around Kraków” (e.g., Kaczanowska and Kozłowski, 1976; Lech, 1980; Přichystal, 2013) and the “chocolate flint” (e.g., Krukowski, 1920; Schild, 1971; Budziszewski, 2008). The occurrence of both flint varieties is suggested to be limited only to local sources. Moreover, the appearance of even individual, several-centimetre-long specimens in artifact inventories has been taken as evidence of contacts between Late Paleolithic-Mesolithic communities over distances that could exceed

500 km (e.g., Sulgostowska, 2005; Mateiciucová and Trnka, 2015; Burgert, 2018; Sudoł-Procyk et al., 2021a).

While the term “Jurassic flint around Kraków” (JFAK) clearly indicates its provenance from the southern part of the Kraków-Częstochowa Upland (S-KCU), the term “chocolate flint” (CF), initially used exclusively for specimens that originated from the northeastern margin of the Holy Cross Mts., has recently been applied also to artifacts collected at archaeological sites in the central KCU (Krajcarz et al., 2012; Krajcarz and Sudoł-Procyk, 2019; Sudoł-Procyk et al., 2018, 2021a, b, 2022; Manderá et al., 2024). Although, to date, the colour of the CF has not been precisely defined as a diagnostic feature (cf. Budziszewski, 2008: p. 47; Manderá et al., 2024), this criterion has been taken to be unambiguously macroscopically identifiable in artifact collections, which can lead to conclusions crucial to interpreting contacts between prehistoric communities throughout Central Europe (cf. Burgert, 2018; Sudoł-Procyk et al., 2021a).

The key criterion for identification of siliceous artifacts in archaeological studies should be their petrographic character-

* Corresponding author, e-mail: kochman@agh.edu.pl

Received: January 30, 2025; accepted: April 1, 2025; first published online: June 16, 2025

ization (e.g., Luedtke, 1979; Skarpelis et al., 2017; Chatzimanologlou et al., 2020). Unfortunately, the vast majority of archaeological research projects focused on the classification of siliceous artifacts in order to determine their provenance have been based exclusively on macroscopic descriptions of their outer surfaces, which are usually rough, commonly weathered and coated with patina. The standard, destructive petrographic methods: observations of thin and polished sections, as well as geochemical analyses, cannot be applied because artifacts must remain undamaged. By contrast, advanced, non-destructive methods, e.g. laser ablation-inductively coupled plasma-mass spectrometry (LA-ICP-MS; cf. Roll et al., 2005; Brandl et al., 2016; Sanchez de la Torre et al., 2017) or mid-infrared spectroscopy (cf. Parish, 2011; Schürch et al., 2022) are still rarely used because of their high cost. However, even these latest methodologies usually do not allow researchers to precisely determine the provenance of artifacts, particularly those derived from carbonate strata of similar development and age.

A critical analysis of the macroscopic identification criteria of both the JFAK and CF in artifact inventories has already been published by Kochman et al. (2020a) and Matyszkiewicz and Kochman (2020). It was demonstrated that it is impossible to assign the origin of any given flint artifact to the Upper Jurassic strata from any specific region of the KCU based solely on macroscopic criteria because similar varieties of siliceous raw materials occur throughout the entire KCU (cf. Kochman et al., 2020b; Kochman and Matyszkiewicz, 2023).

In 2023, comparative studies were initiated in southeastern Bavaria, in the southernmost part of the Franconian Alb (FA) and in the Bayerwald (BW) (Fig. 1). These two regions were selected because: (1) the majority of the Upper Jurassic limestone facies hosting the cherts in both the FA and BW (e.g., Zeiss, 1977, 2012; Meyer and Schmidt-Kaler, 1990; Niebuhr and Pürner, 2014) show a development similar to that known from the KCU (e.g., Dżułyński, 1952; Kutek et al., 1977; Matyszkiewicz, 1997), (2) sites of extraction and processing of siliceous raw materials are known from both southeastern Germany (e.g., Reisch, 1974; Engelhardt, 1985; Weißmüller, 1995; Binstener, 2005, 2013; de Grooth, 1994, 1997; Bertola and Schäfer, 2013; Burgert, 2016), and the KCU (e.g., Kowalski and Kozłowski, 1958; Dagnan-Ginter et al., 1976; Dziędużyska-Machnikowa and Lech, 1976; Ginter, 1980; Sobczyk, 1993; Chochorowska and Dagnan-Ginter, 1995; Wilczyński, 2016), (3) potential export of siliceous raw materials and finished goods from the source regions should have proceeded also towards Bohemia and Moravia, located roughly midway between the KCU and the FA/BW (Fig. 1A).

Artifact inventories in Bohemia and Moravia include few, or individual, chert artifacts labeled JFAK (e.g., Kozłowski, 1958; Vencel, 1971; Kaczanowska and Kozłowski, 1976; Přichystal, 1985; Lech, 1993; Oliva, 2001, 2007; Voláková, 2001; Janák and Přichystal, 2007; Nerudová and Přichystal, 2011; Šebela et al., 2017 and others) or CF (e.g., Vencel, 1978; Lech, 1989; Vávra, 1993; Oliva, 2001; Voláková, 2001; Přichystal and Šebela, 2009; Čuláková, 2015; Burgert, 2018; Přichystal, 2018 and others). Moreover, there are also documented artifacts allegedly sourced in the FA/BW (e.g., Pleslová-Štiková, 1969; Vencel, 1971; de Grooth, 1995; Binstener, 2001, 2005, 2013; Trnka, 2004; Mateiciucová, 2008; Burgert, 2016). As the identification of artifacts in these cited publications was based exclusively on macroscopic descriptions and analyses, we ask: do there exist any macroscopic criteria which would unambiguously identify the provenance of any given siliceous artifact?

GEOLOGICAL SETTING

In the Late Jurassic, the KCU and the FA/BW regions occupied the northern shelf of the Tethys Ocean where carbonate sedimentation prevailed as the “microbial-sponge megafacies” (e.g., Gwinner, 1971, 1976; Keupp et al., 1990; Matyszkiewicz, 1999). Identical factors controlling biogenic sedimentation resulted in significant similarity of development of Upper Jurassic successions exposed between Portugal and the Caucasus Mts. This is the case for massive (non-bedded) facies, i.e. microbial-sponge, microbial and coral buildups, which are practically devoid of cherts, as well as for normal (bedded) facies, which locally host cherts distributed parallel to the bedding surfaces or, less commonly, randomly scattered within the rock body.

The most important differences in development of Upper Jurassic strata in both the KCU and the FA are: (1) a thicker succession preserved in the FA (>400 m), by comparison with the KCU (~300 m), (2) a related wider stratigraphic range of the succession in the FA (Oxfordian-Lower Tithonian), in comparison with the KCU (Oxfordian-Lower Kimmeridgian), (3) the common occurrence of dolomitization in Upper Jurassic limestones in the FA whereas in the KCU dolomitization appears only locally, in the uppermost part of succession.

In both regions, bedded limestones are represented mostly by microbial-sponge biostromes (e.g., Dżułyński, 1952; Matyszkiewicz, 1989; Keupp et al., 1990; Brachert, 1992; Krajewski et al., 2018; Kochman et al., 2020a; Matyszkiewicz and Kochman, 2020), which locally host chert concretions. The second, specific silicification products are bedded cherts, which are observed in the fine-grained deposits of submarine gravity flows, the “alldapic limestones” (cf. Meischner, 1964). In the FA, such deposits are described as “Kieselplatten” or “Plattensilex” (e.g., Rutte, 1962; v. Freyberg, 1964, 1968; Weber, 1978; Kleinschnitz, 2001; Meyer, 2003a, b) whereas in the KCU, the name “bedded cherts” is in common use (Matyszkiewicz, 1996; Matyszkiewicz and Kochman, 2020).

In the southeastern part of the FA studied (Fig. 1B), both chert concretions and thin-bedded cherts are observed, mostly in the Tangrintel Formation (Upper Kimmeridgian-Lower Tithonian) (cf. Rutte, 1962; Weber, 1978; Meyer, 1977; Binstener, 2005; Niebuhr and Pürner, 2014). Less common are chert concretions in the Treuchtlingen Formation (upper part of the Lower Kimmeridgian-middle part of the Upper Kimmeridgian) (Meyer, 1975, 2003c; Niebuhr and Pürner, 2014) and in the Painten Formation (bottom part of the Lower Tithonian) (Streim, 1961; Niebuhr and Pürner, 2014) whereas thin-bedded cherts are known from the Torleite Formation (middle-topmost parts of the Upper Kimmeridgian) (Streim, 1961; Zeiss, 1964; Binstener, 2005; Niebuhr and Pürner, 2014).

The Upper Jurassic strata of the BW are different. These are relicts of an Upper Jurassic succession which represents the stratigraphic interval from the Middle Oxfordian to the Lower Kimmeridgian (so-called Ortenburg Formation) (cf. Zeiss, 1977; Meyer, 1977; Gröschke, 1985; Niebuhr, 2014) and comprise thick-bedded limestones with numerous chert concretions. These deposits reveal a distinct similarity to the Upper Jurassic bedded limestones of the KCU, particularly of the S-KCU.

MATERIALS AND METHODS

The methodology applied in this research project included collecting 37 rock samples from 5 exposures located in the southern FA and in the BW (Fig. 1). The stratigraphic position of

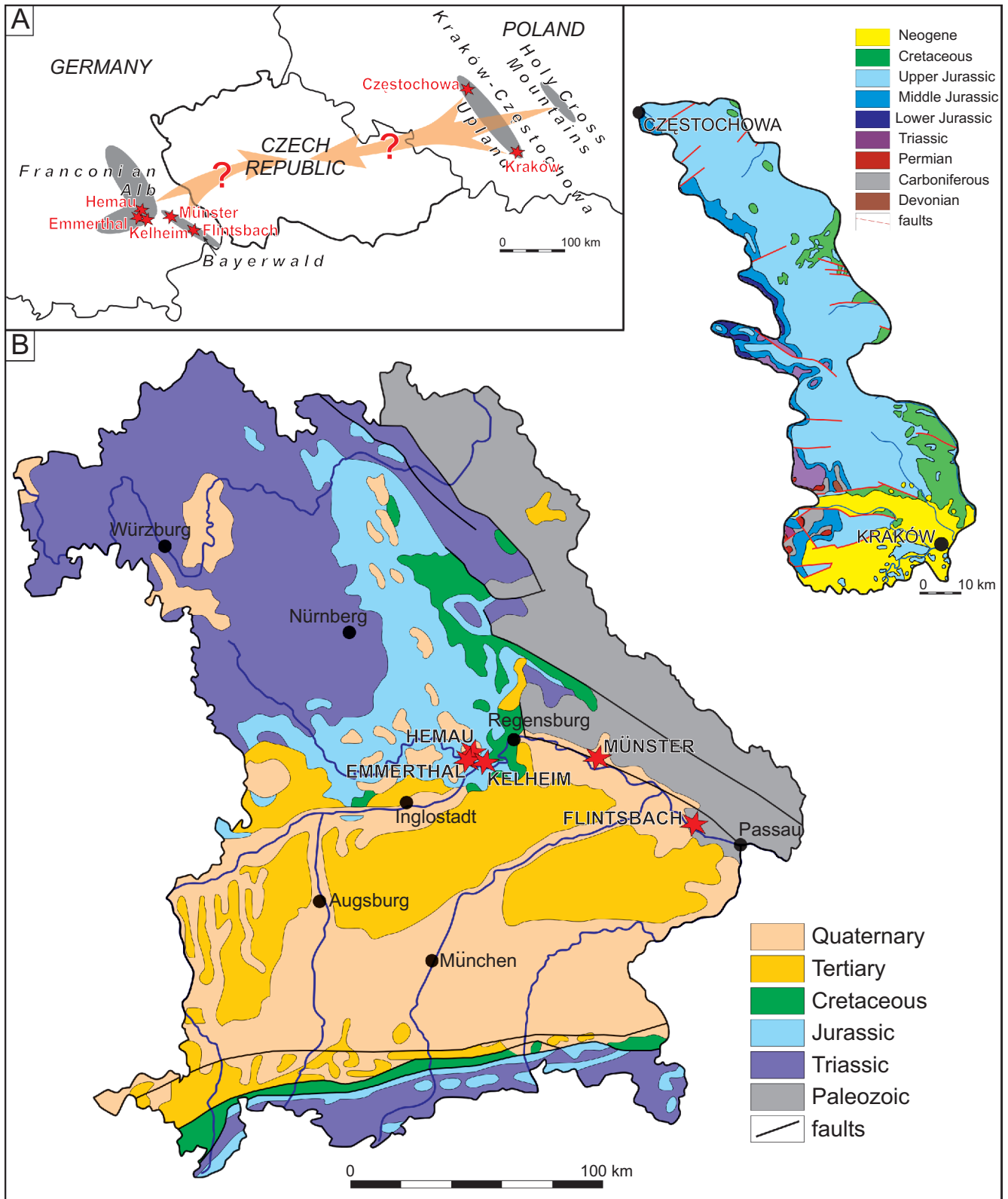


Fig. 1. Location of study area

A – possible export directions of siliceous raw materials and finished products in the Paleolithic, Mesolithic and Neolithic from Poland (Kraków-Częstochowa Upland and NE margin of the Holy Cross Mts.) and SE Germany (Franconian Alb and Bayerwald). The area of Bohemia where artifacts said to originate from Poland or Germany were found is located halfway between these two areas of intensive mining and processing of siliceous raw materials. Location of the KCU on the Geological Map of Poland (Rühle et al., 1977). **B** – sampling sites referred to on a simplified Geological Map of Bavaria. Emmerthal, Kelheim and Hemau sites are located in the Franconian Alb; Münster and Flintsbach belong to the Bayerwald, where relicts of Upper Jurassic successions are preserved (not shown on the map due to their small scale; after Doben et al., 1996, simplified)

the sampled exposures was taken from the 1:25 000 scale Geological Map of Bavaria with explanations. Names of stratigraphic units are based upon Niebuhr and Pürner (2014), and Niebuhr (2014).

In the southern FA, samples were collected from 3 exposures, among which Emmerthal represents the Torleite Formation whereas Hemau and Kelheim comprise strata from the Tangrintel Formation. In the BW, exposures were sampled at the Münster and Flintsbach sites, both representing the Ortenburg Formation (Fig. 1).

During the field sessions, each chert sample was taken together with the enclosing limestone, with the way-up being marked, enabling sedimentological analyses of the cherts together with their hosting limestones. Additionally, field observations were supported by photographic documentation of all sampling sites and their GPS coordinates. From the collected samples, 30 polished sections (Emmerthal – 4, Kelheim – 8, Hemau – 4, Münster – 8, Flintsbach – 6) and 80 thin-sections (Emmerthal – 9, Kelheim – 20, Hemau – 8, Münster – 25, Flintsbach – 18) were prepared and examined for microfacies analysis using an *Olympus SZX10* polarizing microscope. For a single chert concretion from the Kelheim exposure, which a revealed spectacular diversity of colours, the ^{57}Fe Mössbauer spectrum was recorded at room temperature in order to confirm its multi-stage formation process and diverse silica sources. Spectrometry in transmission geometry was carried on with a *RENON MsAa-4* spectrometer equipped with a LND Kr-filled proportional detector and $^{57}\text{Co(Rh)}$ source (Błachowski et al., 2008). For the remaining samples it was not possible to quantify the presence of Fe.

Comparative materials originated from the inventory of thin and polished sections of siliceous rocks collected from the Upper Jurassic successions across the entire KCU and stored at the Department of Environmental Analysis, Geological Mapping and Economic Geology, Faculty of Geology, Geophysics and Environment Protection, AGH University of Science and Technology in Kraków. In total, 49 comparative samples were used, taken from 7 exposures located in the S-KCU and from 1 exposure in the N-KCU. Among these, 23 samples represent chert concretions and 26 are bedded cherts. Detailed petrographic descriptions of siliceous rocks from the KCU have already been published by Kochman et al. (2020a, b), Matyszkiewicz and Kochman (2020) and Kochman and Matyszkiewicz (2023); hence, only brief characterizations of the chert concretions and bedded cherts are provided below.

Geochemical analysis of samples collected from the Franconian Alb, Bayerwald, and Kraków-Częstochowa Upland has been conducted, and the results will be presented in forthcoming publications.

PETROGRAPHY OF CHERTS FROM THE FRANCONIAN ALB AND THE BAYERWALD

FRANCONIAN ALB

EMMERTHAL – TORLEITE FM.; INACTIVE QUARRY NEAR PRUNN
(GPS: 48°57'39.00"N, 11°43'00.00"E)

Macroscopic features

In an intermittently worked quarry near Prunn (Fig. 2), where the walls are ~20 m high, thick-bedded limestones are



Fig. 2. Emmerthal Quarry

A – main wall exposing bedded, locally dolomitized limestones with chert concretions; in the upper part of the quarry, intense karst features are seen; B – light-cream, ellipsoidal chert concretion hosted in dolomitized limestone

exposed, in which individual layers are up to ~2.5 m thick (Fig. 2A). The weathered limestone surfaces are grey whereas the fresh fractures are light brown. In the upper parts of the quarry walls, the limestones are strongly karstified.

On weathered limestones surfaces, cream-coloured casts of siliceous sponges and chert concretions were observed (Fig. 2B), mostly horizontally arranged. Both the cherts and sponges (Figs. 2B and 3A, E), as well as single brachiopods and bivalves, distinctly protrude from the rock matrix. The limestones are developed as wackestones-packstones with intercalations of boundstone (terminology after Dunham, 1962).

The chert concretions vary in shape. Most common are ellipsoids (Figs. 2B and 3A, C, E) but spheres and irregular forms are also present. Their diameters may exceed ten centimetres (along the longer axis) but are usually up to several centimetres. The cores of concretions are mostly casts of siliceous sponges (Fig. 3A, C). Colours are diverse: the central parts are brownish-grey whereas towards the outer parts, the colour grades to almost white (Fig. 3A, C, E).

Microscopic observations

Under the microscope, the limestones commonly show unitary sedimentary sequences (Gaillard, 1983; Matyszkiewicz, 1989) formed by siliceous sponges (Fig. 3D) with microbialites developed onto their upper surfaces and epifauna (mostly bryozoans and polychaetes) settled on the bottom surface. The sediment between the sponge bodies is a wackestone-packstone with individual bryozoans (Fig. 3B) and brachiopod specimens. Locally, the limestone is dolomitized (Figs. 3F and 4A, C, D). In some limestone samples, dolorhombs are dissolved at the contact with the chert concretion (Fig. 4A) producing a mouldic porosity, but most of the dolorhombs remain unaffected (Figs. 3F and 4C, D).

The chert concretions are silicified patches of limestone. Usually, the cores of concretions are formed by skeletons of Hexactinellida siliceous sponges (Fig. 3D). The contours of bioclasts are filled with both chalcedony (Fig. 4B) and granular quartz. Sporadically, the relics of non-silicified fauna occur. The carbonate matrix is replaced by cryptocrystalline silica. The limestone/chert boundaries locally follow stylolites (Fig. 4A, C, D).

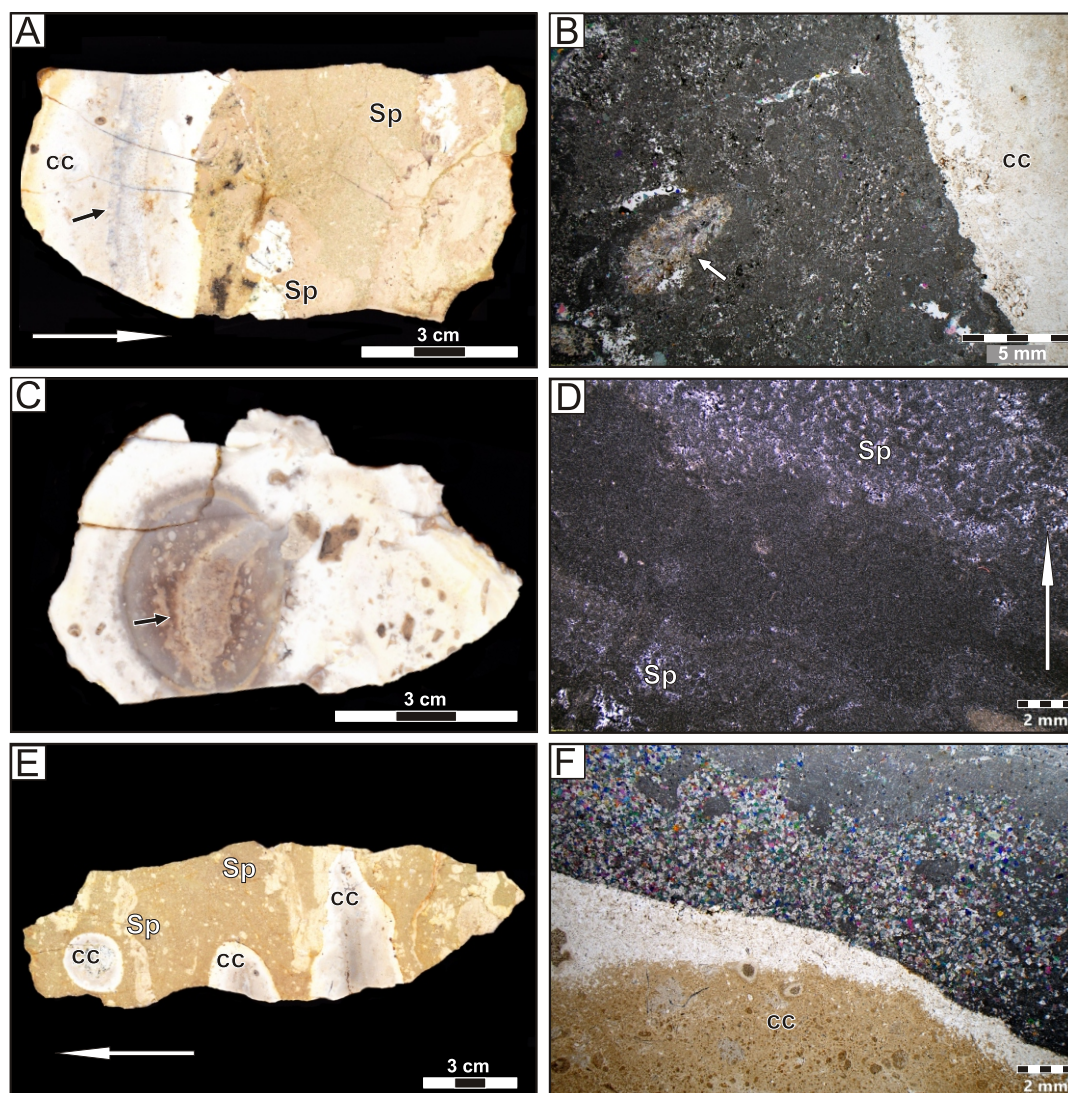


Fig. 3. Photographs of polished – A, C, E and thin (B, D, F) sections (Emmerthal Quarry)

A – limestone with chert concretion (cc) and silicified casts of siliceous sponges (Sp). Siliceous sponge skeleton occupies centre of concretion (black arrow). White arrow indicates direction to the top. **B** – contact of chert concretion (cc) and limestone (wackestone) with individual bioclasts. Arrow marks partly silicified bryozoan fossil. Plane polarized light. **C** – chert concretion with sponge cast in the centre (arrow). Colour becomes increasingly lighter towards the concretion's edge. **D** – chert concretion with recognizable skeletal fragments of siliceous sponges (Sp). Arrow indicates direction to the top. Crossed polars. **E** – partly dolomitized limestone with chert concretions (cc) and casts of siliceous sponges (Sp). Arrow indicates direction to the top. **F** – contact of chert concretion (cc) with dolomitized limestone. Close to the contact, the limestone contains numerous euhedral dolomite crystals completely replacing calcite. Dolomitization is selective: dolomite crystals occur only in the matrix whereas irregular oncoids remain unreplaced. Plane polarized light

Interpretation of depositional and diagenetic environments

The bedded limestones are interpreted as the early development stages of typical biostromes representing the microbial-sponge megafacies. Dolomitization and partial dedolomitization processes proceeded prior to pressure solution, which produced stylolites and dissolution seams. The boundaries of chert concretions located on stylolites indicate that silicification was a late-diagenetic process, which followed chemical compaction.

KELHEIM – TANGRIINTEL FM.; EXPOSURE BY THE PATH
(GPS: 48°54'54.40"N, 11°55'20.60"E)

Macroscopic features

Limestones with chert concretions and thin-bedded cherts occur in an exposure ~5 m high and 8 m long, located on the northern side of a country road. The lower part of that section comprises thin-bedded limestones with graded bedding (Fig. 5). In the coarser-grained layers, faunal detritus is observed. The overlying nodular limestone (Fig. 5) contains abundant bivalves, corals and brachiopods.

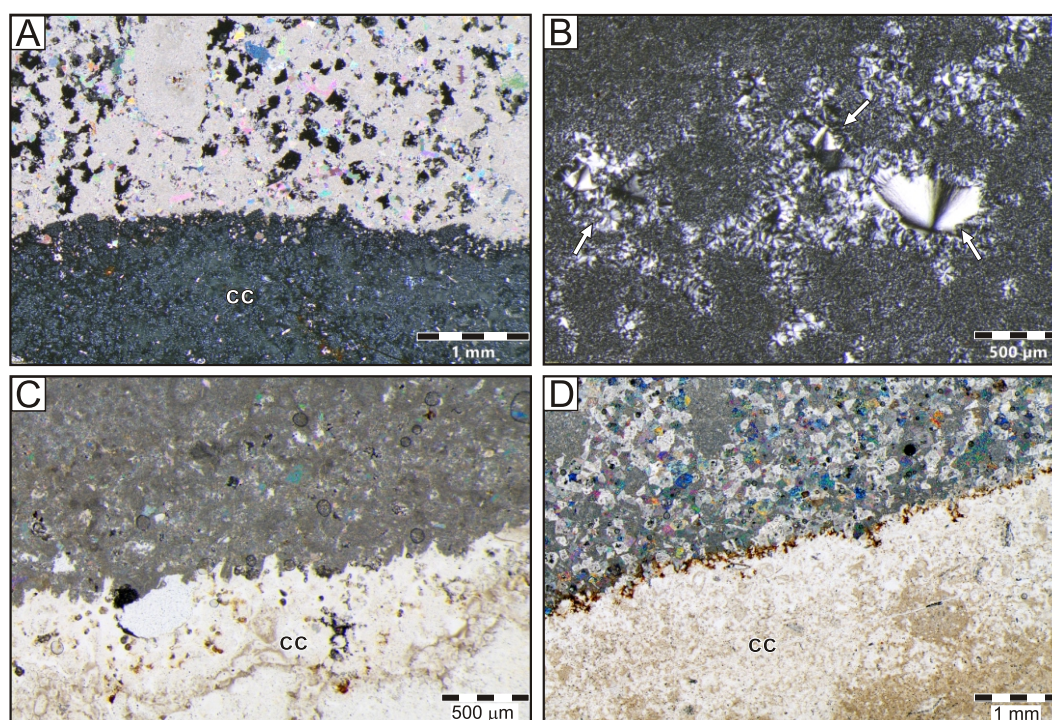


Fig. 4. Microfacies development of chert concretions (Emmerthal Quarry)

A – contact of chert concretion (cc) with limestone along stylolite. Euhedral dolomite crystals in the limestone were partly dedolomitized producing mouldic porosity. Crossed polars. **B** – fragment of secondarily silicified skeleton of hexactinellid siliceous sponge replaced by granular quartz and chalcedony (arrows). Crossed polars. **C** – contact of chert concretion (cc) with limestone along stylolite. Limestone contains individual, euhedral dolomite crystals. Plane polarized light. **D** – contact of chert concretion (cc) with intensely dolomitized limestone along stylolite impregnated with brownish Fe-oxides. Plane polarized light

Silicification products are present in both the thin-bedded and the nodular limestones. In the former, tabular, thin-bedded cherts (Figs. 5 and 6A, B) occur together with ellipsoidal chert concretions (Figs. 5 and 6C, D). By contrast, in the nodular limestones, concretions reveal irregular shapes (Figs. 5 and 6E, F). The most intense silicification proceeds at the contact



Fig. 5. Kelheim exposure

in the lower part, limestones (tempestites) with individual, silicified layers of thin-bedded cherts are exposed (so-called *Plattensilex*; black arrows); in the upper part, nodular limestones (debris flows) with irregular chert concretions (white arrows) are seen

between thin-bedded and nodular limestones where massive, multicoloured, rounded concretions occur (Fig. 6E).

The thickness of the thin-bedded chert layers varies from ~1 to 5 cm. Thicker (3–5 cm), brownish thin-bedded cherts with flat top and bottom surfaces (Fig. 6A) are built of homogenous, fine-grained rock, in which irregular spots are scattered. These are presumably burrows made within the fine-grained material prior to silicification. Thinner (~1–2 cm) detrital laminae are brownish in colour, contain silicified fossil fragments and show somewhat blurred graded bedding (Fig. 6B). Top and bottom surfaces of these laminae are usually smooth, some being wavy.

The ellipsoidal concretions hosted in the thin-bedded limestones may exceed 10 cm along their long axes whereas their width does not exceed 5 cm. Their internal structure is concentric with cortices built of bands up to ~1 cm thick (Fig. 6C). Usually, individual bands reveal subtle differences in colour. In places, their cores are coated by internal bands of brownish ("chocolate"?) silica whereas the outer bands are greyish-white or brownish (Fig. 6D).

The chert concretions observed in nodular limestones, close to the contacts with thin-bedded cherts, are large (up to ~20 cm in diameter) and show diverse colours. Their cores, up to 15 cm across, are built of multicoloured, spotty chert full of clearly visible fragments of bivalves, brachiopods, siliceous sponges and gastropods. Such cores are coated with cortical bands of total thickness up to ~5 cm (Fig. 6E), usually lighter in colour than the core.

Occasionally, concretions collected from the nodular limestones do not have distinct cores and cortices (Fig. 6F). These

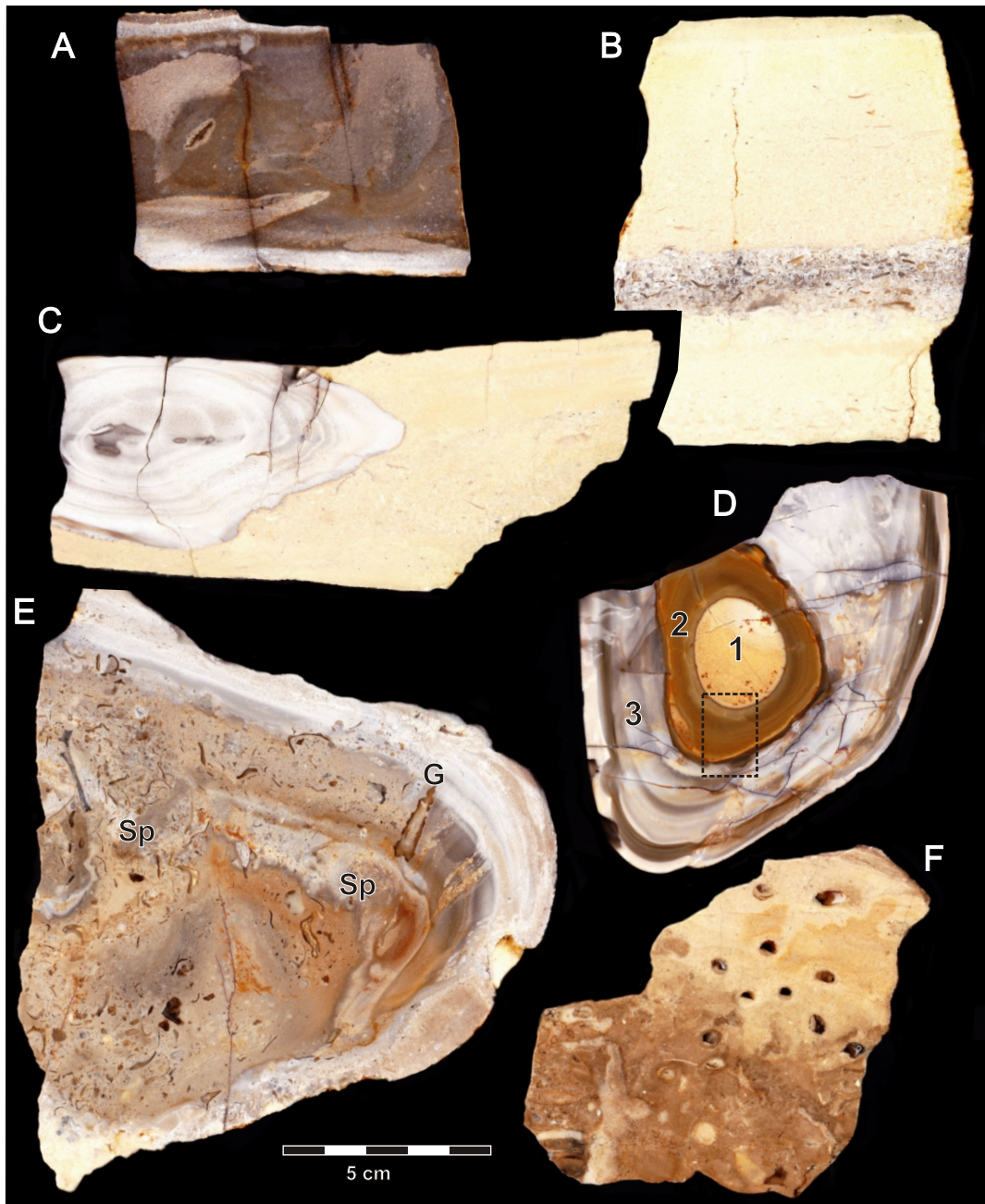


Fig. 6. Photographs of polished sections of chert concretions and tabular cherts (Kelheim exposure)

A – tabular chert with flat top and bottom surfaces. Perpendicular joints are filled with brownish Fe-oxides. The spotted structure is related to burrows in the carbonate sediment, subsequently silicified. **B** – an individual tempestite, in which both the fine bioclasts and the enclosing matrix are silicified. The silicified tempestite shows poorly marked graded bedding. **C** – chert concretion from the tempestite succession with concentric, banded structure. **D** – tripartite chert concretion from the tempestite succession close to its contact with nodular limestone. The regular, almost perfectly spherical core (1) is enclosed in a brownish ("chocolate"?) envelope (2) followed by light-grey and brownish silica bands (3) of the cortex. Area in rectangle is shown in [Figure 7D](#). **E** – chert concretion with massive, light-brownish, spotted core, in which casts of siliceous sponges (Sp) occur together with gastropods (G) and other, fine bioclasts. The core is enveloped by a thin-banded cortex. **F** – fragment of chert concretion from nodular limestone. In the upper, light-brownish part, a silicified fragment of coral occurs whereas the bottom part is formed by silicified sediment with numerous fragments of thick-shelled bivalves. No distinct cortex is observed

are irregular fragments of brownish, silicified limestone with clearly visible relics of silicified corals, bivalves and brachiopods.

Microscopic observations

The thin-bedded limestones represent tempestites with well-developed sorting and graded bedding. Thin-bedded cherts of thickness from 3 to 5 cm are developed as silicified, graded-bedded mudstones-wackestones (Fig. 7A). Burrows in primary mudstones are filled with wackestone. In such deposits, the limestone/chert contacts are even and sharp.

Thinner (1–2 cm), silicified laminae are packstones-grainstones of grain size up to ~2 mm (Fig. 7B). Their top and bottom

surfaces are uneven and silica protrusions penetrate into the over- and the underlying limestone to a distance of ~1 mm.

In the chert concretions hosted in thin-bedded limestones, both silicified mudstones-wackestones and packstones-grainstones were observed. Boundaries of the chert concretions are oblique to the sedimentary lamination produced by graded bedding (Fig. 7C).

In places, in the finest-grained, best-sorted tempestites, multicoloured cortical bands do not show differences in development of carbonate sediment later subjected to silicification (Fig. 7D). Boundaries of bands having different colours are usually emphasized by the presence of brownish Fe-oxides (Fig. 7D).

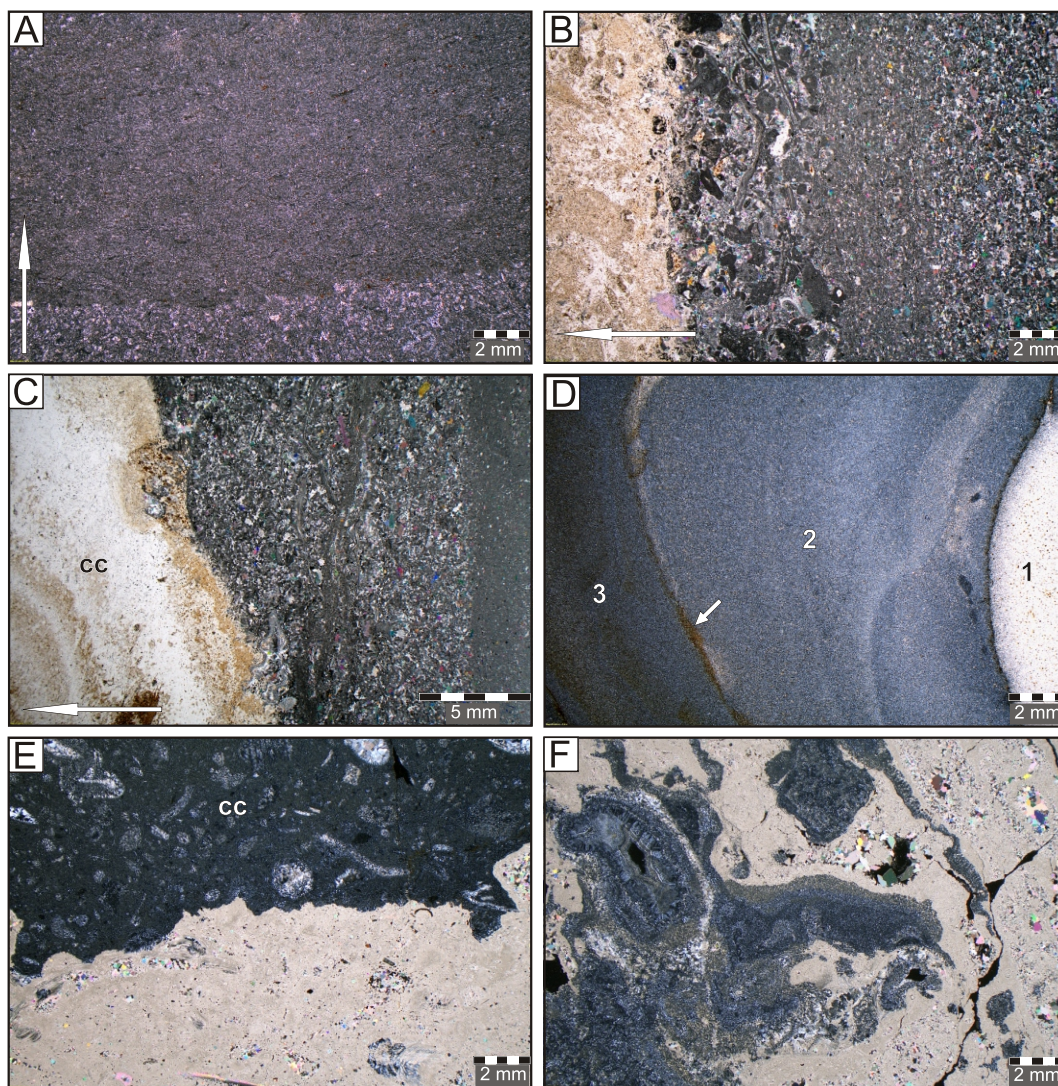


Fig. 7. Microfacies development of chert concretions and tabular cherts (Kelheim exposure)

A – tabular chert having even top and bottom surfaces, and homogenous, silicified laminae of similar grain size. Arrow indicates direction to the top. Crossed polars. **B** – contact of limestone developed as tempestite succession with a single, silicified tempestite lamina. Laminae differ in grain size. Arrow indicates direction to the top. Plane polarized light. **C** – contact of chert concretion (cc) with limestone developed as a tempestite succession. Lamination of tempestite results from variation in grain size. Limestone/chert concretion boundary is oblique to horizontal lamination. Arrow indicates direction to the top. Plane polarized light. **D** – microscopic image of chert concretion from Figure 6D. Core (zone 1) is visible on the right, “chocolate” chert (zone 2) is on the left and cortex bands (zone 3) appear on the extreme left. The sediment in all three zones is a mudstone. Boundary between zones 2 and 3 is marked by Fe-oxides (arrow). Crossed polars. **E** – boundary between chert concretion (cc) and nodular limestone representing a debris flow deposit. Concretion shows contours of bioclasts filled with granular quartz. Crossed polars. **F** – irregular aggregates of silica in nodular limestone (debris flow). Crossed polars

The nodular limestones are developed as packstones-grainstones with abundant faunal assemblages of echinoderms (echinoid spines and plates), bivalves, brachiopods, corals and serpulids. Oncoids up to 1 cm across are also common; their cores are fragments of thin-shelled bivalves. Cherts hosted in the nodular limestones reveal sharp and usually uneven boundaries with the enclosing limestone (Fig. 7E). Moreover, irregular aggregates of silica commonly impregnate these limestones (Fig. 7F).

Application of Mössbauer spectroscopy

Application of precise Mössbauer spectroscopy methodology allowed quantification of Fe in the chert concretions studied (Figs. 6D and 7D) from the Kelheim exposure (Fig. 8). The measurements revealed that the spectral component (sextet) with the hyperfine magnetic field B , present only in the P-2 sample, i.e. in the brownish ("chocolate") envelope, belongs to Fe atoms in superparamagnetic nanoparticles of Fe-oxide (hematite) and/or oxyhydroxide (goethite). The spectral component (doublet) without the magnetic hyperfine field present in all three samples analysed probably belongs to Fe atoms hosted in clay minerals and/or to traces of Fe incorporated in SiO_2 . A sample taken from the brownish envelope distinctly differs from those from the core and outer cortex. It contains ~60% of Fe-oxide (hematite) and/or Fe-oxyhydroxide (goethite), which is absent from the remaining samples. Such a distribution of Fe-oxide suggests that: (1) different parts of the chert concretion formed in different chemical regimes, (2) silicification was multistage and (3) silica was supplied from various sources.

Interpretation of depositional and diagenetic environments

The thin-bedded limestones from the lower part of the Kelheim exposure are interpreted as tempestites formed during redeposition of detrital material from the shallower parts of the sedimentary basin. By contrast, the overlying nodular limestones are products of debris flows. Redeposition of sedimentary material indicates the presence of topographic variations on the basin floor. The uplifted zones originated from aggradational growth of carbonate buildups, the upper parts of which were settled by shallow-water fauna assemblages. The areas between the carbonate buildups (so-called "Wannen"; cf. Meyer, 1977) were located at greater depths.

The formation of thin-bedded cherts was a late-diagenetic process that selectively replaced specific parts of the tempestite succession. The chert concretions hosted in both the tempestites and the debris flow deposits were similarly late-diagenetic. Contrasting colours observed in some chert concretions resulted from multistage silicification and various sources of silica.

HEMAU – TANGRIINTEL FM.; SILICEOUS REGOLITH
(GPS: 49°02'34.90"N, 11°44'19.00"E)

Macroscopic features

Samples were collected from a weathering zone developed in a forested area. The enclosing limestone has not been preserved whereas the cherts occur as fragments of tabular, thin-bedded and concretionary geometrical varieties (Fig. 9A, C, E).

The thin-bedded cherts are light-brown, tabular, distinctly laminated bodies, up to 4 cm thick (Fig. 9A). The thicknesses of individual laminae reach up to 1 cm but most common are those up to several millimetres thick. Another variety comprises

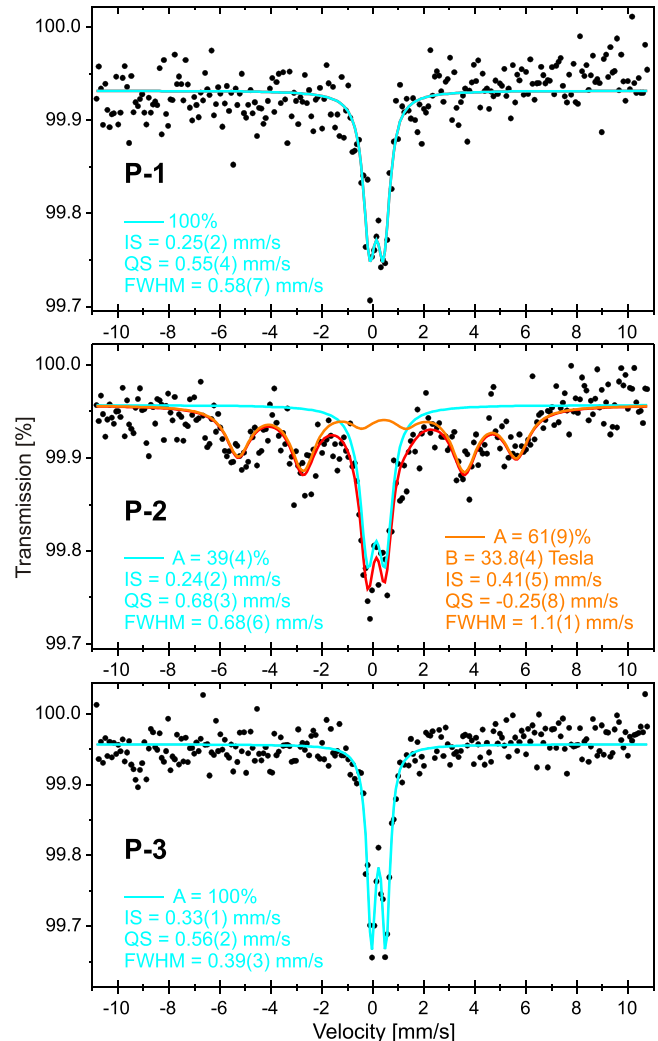


Fig. 8. ^{57}Fe Mössbauer spectra of chert concretion measured at room temperature (Kelheim exposure)

Mössbauer spectroscopy symbols are as follows: A – relative area of spectral components, B – hyperfine magnetic field, IS – isomer (centre) shift relative to $\alpha\text{-Fe}$, QS – quadrupole splitting, and $FWHM$ – spectral line width. Errors are shown in brackets. The relative area A corresponds to distribution of Fe atoms in a specific chemical surrounding, crystallographic site or mineral phase

laminae with black spots <0.2 mm across, randomly scattered within the rock. Sets of parallel laminae are most common (Fig. 9A) but convolute laminations are also present (Fig. 9C).

The chert concretions are usually spherical, up to 10 cm in diameter. Their cores are blurred, as are the cortices, which is presumably the effect of weathering, signs of which are visible on the outer surfaces of concretions. On polished sections, scattered casts of siliceous sponges can be identified together with brachiopod shell fragments (Fig. 9E).

Microscopic observations

Under the microscope, the thin-bedded cherts are built of pale homogeneous laminae, which represent silicified mudstones-wackestones with fine, unidentifiable fossil detritus. La-

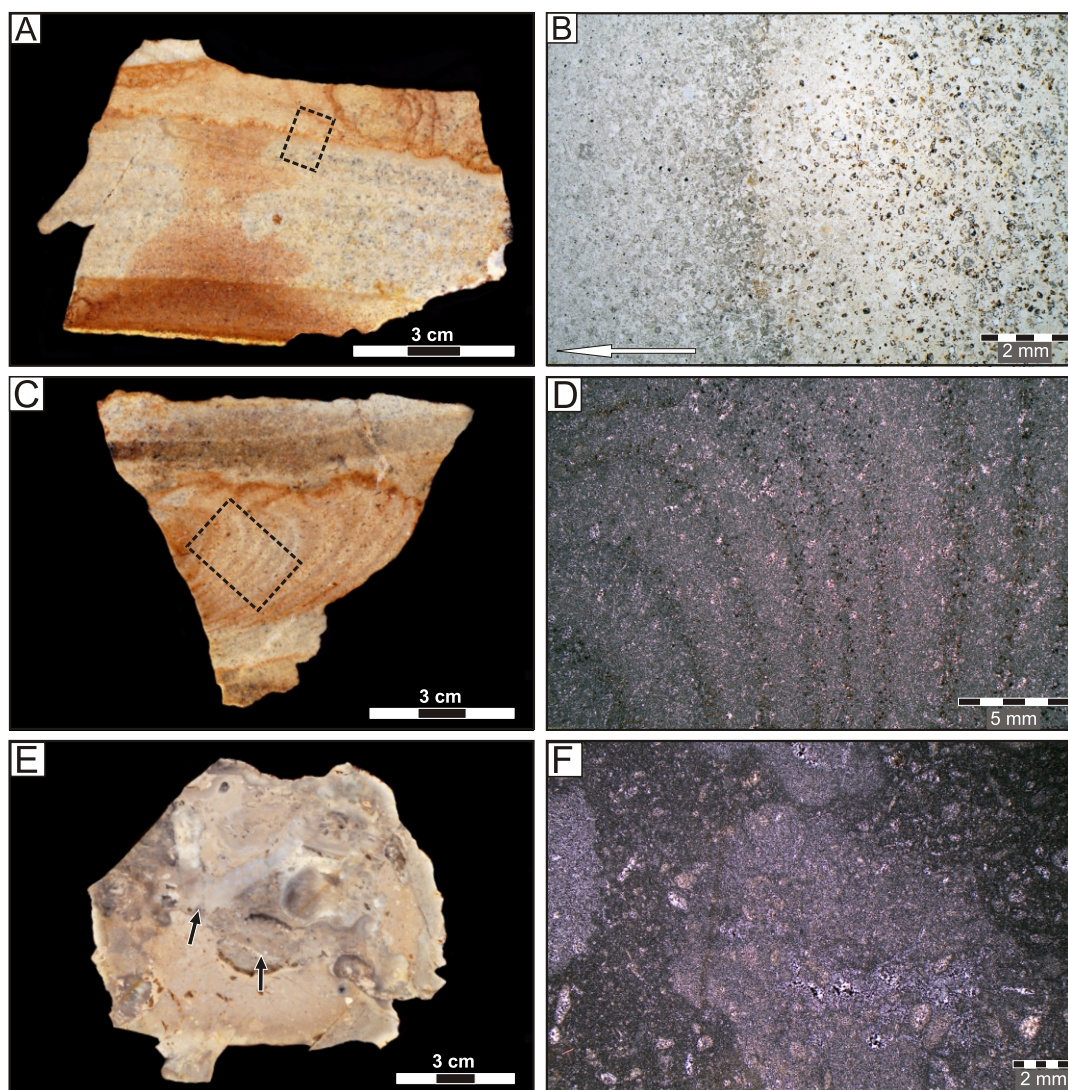


Fig. 9. Photographs of polished (A, C, E) and thin (B, D, F) sections of tabular cherts and chert concretions collected from regolith (Hemau exposure)

A – tabular chert with flat top and bottom surfaces. In the central part, laminae with dark spots are visible, which are absent from the topmost and bottommost parts of this chert. The area in the rectangle is shown in Figure B. **B** – contact of lamina hosting numerous pseudomorphs after dolorhombs, some of them filled with dark Fe-oxides (on the right), with lamina that has not been dolomitized prior to silicification (on the left). Arrow indicates direction to the top. Plane polarized light. **C** – tabular chert, in which the central part is convolutedly disturbed whereas both the topmost and the bottommost parts remain undisturbed. Area in rectangle is shown in Figure D. **D** – convolutedly disturbed lamination with darker laminae containing abundant pseudomorphs after dolorhombs filled with dark Fe-oxides. Crossed polars. **E** – chert concretion, in which only the core was preserved whereas cortex bands were presumably removed by weathering. Spotted core hosts fragments of sponge casts (arrows) and fine, unidentifiable bioclasts. **F** – chert concretion developed as wackestone with abundant, unidentifiable fossil fragments. Crossed polars

minae with dark spots are wackestones with abundant rhombohedral pseudomorphs after dolomite, now partly filled with dark Fe-oxides (Fig. 9B). Selective dedolomitization of laminae is observed also in convolute structures (Fig. 9D).

The chert concretions are silicified packstones-grainstones, locally also boundstones with sponge casts and tuberoids (Fig. 9F), as well as microbialites developed on casts of siliceous sponges.

Interpretation of depositional and diagenetic environments

The thin-bedded cherts are interpreted as silicified tempestites deposited onto the sloping surface of a tidal flat. Alternating, dolomitized and non-dolomitized laminae with convolute disturbances indicate early diagenetic dolomitization, which proceeded after deposition of the laminae but prior to their lithification and generation of convolute disturbances, whereas the silicification was a late-diagenetic process.

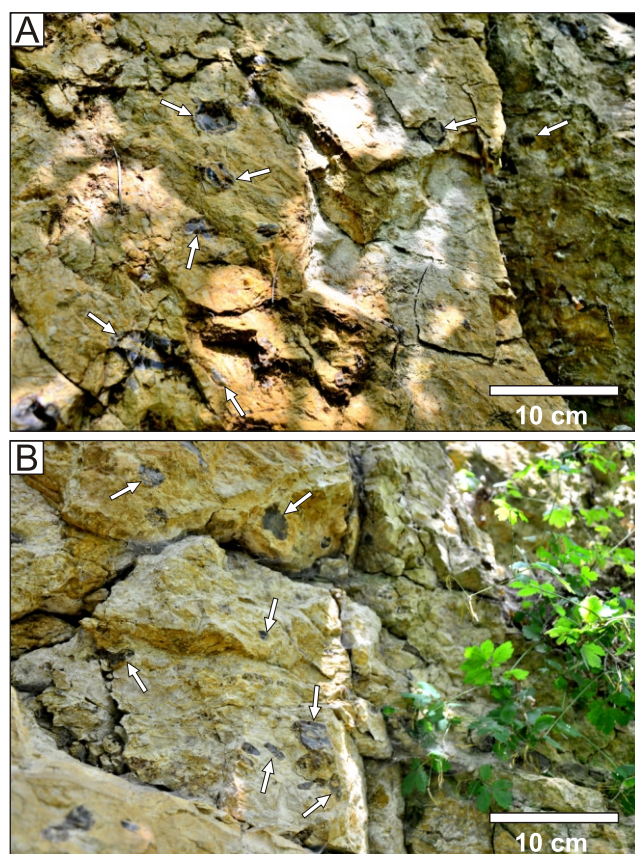


Fig. 10. Part of the section exposed (Münster exposure)

A, B – chert concretions (arrows) randomly distributed within the limestone

BAYERWALD

MÜNSTER – ORTENBURG FM.; SMALL EXPOSURE
(GPS: 48°56'53.62"N, 12°34'08.17"E)

Macroscopic features

The samples were collected in an abandoned, densely vegetated quarry, several metres high and long, located in a forest (Fig. 10A, B). In the walls, cream, locally light-brown, poorly bedded biostromal limestones are exposed with numerous casts of siliceous sponges and scattered echinoid spines. Siliceous concretions, that can exceed ten centimetres across, are common.

The chert concretions are randomly distributed within the limestones (Fig. 10A, B). Their shapes are diverse: spherical, ellipsoidal and irregular (Fig. 11A, F). Individual concretions have cores enveloped by white cortices up to 5 mm thick. The cores vary in colour, having light-grey centres and darker contacts with the cortices. Moreover, aggregates are observed composed of 2–3 cores enclosed in a common cortex (Fig. 11C, D). Sporadically, the cores comprise brownish spots distributed randomly or aligned along fractures (Fig. 11A–D). Within the cores, casts of siliceous sponges are common, with microbialites that grew on their upper surfaces and epifauna that settled on bottom surfaces (Fig. 11A, B, E, F). Small (up to a few centimetres across) concretions are built of only single, silicified sponges but the silicification does not affect either the microbialites on the upper surfaces or epifauna on their bottoms (Fig. 11F).

Microscopic observations

The limestone host of the chert concretions is a boundstone with numerous unitary sedimentary sequences built of siliceous sponges (Fig. 12A, B). Their upper surfaces are covered by microbialites whereas the bottom ones were settled by epifauna. Spaces between the sponge skeletons are filled with wackestone-packstone with scattered dolomite crystals (Fig. 12C, D). Locally, the dolorhombs were dissolved and mouldic porosity developed (Fig. 12C). Dolomitization proceeded also along stylolites that could be partly filled with Fe-oxides (Fig. 12E, F).

The chert concretions are of silicified limestone. Their cores are usually occupied by casts of hexactinellid siliceous sponges (Fig. 12B). The enclosing wackestones-packstones are almost completely replaced by cryptocrystalline silica, whereas the relics of single, larger bioclasts are replaced by granular quartz. The sponge skeletons are filled with chalcedony or granular quartz. In places, in their peripheral parts, the skeletons are filled with calcium carbonate (Fig. 12D).

Interpretation of depositional and diagenetic environments

The biostromal bedded limestones with chert concretions and casts of siliceous sponges are interpreted as typical sediments of the microbial-sponge megafacies. Two stages of dolomitization are inferred in these deposits: (1) an early stage represented by dolomite crystals scattered within the sediment, which were then locally dedolomitized and (2) a late stage related to dolomitization advancing along stylolites partly filled with Fe-oxides. Generally, the silicification was a late-diagenetic process.

FLINTSBACH – ORTENBURG FM.; SMALL, INACTIVE QUARRY
(GPS: 48°42'53.49"N, 13°06'29.61"E)

Macroscopic features

The samples were collected from an abandoned quarry, ~4 m high and about ten metres wide. In the quarry walls, light-cream bedded limestones are exposed (Fig. 13A). These are wackestones-packstones with casts of siliceous sponges accompanied by individual brachiopods and *Crescientella* sp. Individual beds vary in thickness from some tens of centimetres to over 1 m. The limestones host individual, irregular chert concretions with diameters up to ~10 cm (Fig. 13B, C). Both ellipsoidal and the irregular, branching concretions were observed (Fig. 14A). Based on their colour and geometry, two types of concretion are evident.

The first type is dark-grey though the colour grades into light grey towards the peripheries of particular specimens (Figs. 13B and 14A, B). However, the inverse relationship can also be found. The only identifiable components are casts of siliceous sponges. Cortices are white, up to 1 cm thick and usually discontinuous as they cover only some parts of the cores (Fig. 14A). Some concretions are aggregates of several individuals that may reach up to 10 cm across (Fig. 14A).

The second type is light grey only in the centre whereas peripheral parts are light-cream or even white, with irregular, brownish-cherry spots (Figs. 13C and 14C, D) and randomly distributed dark spots up to 2 mm across (Fig. 13C). The shapes are spherical or ellipsoidal, cores are absent and the bodies are strongly fractured. Their outer surfaces are locally covered with rusty-brown coatings, up to ~1 mm thick. Diameters of these concretions usually do not exceed 5 cm.

Microscopic observations

The limestone hosts are wackestones-packstones, locally also boundstones. Bioclasts include echinoderm fragments,

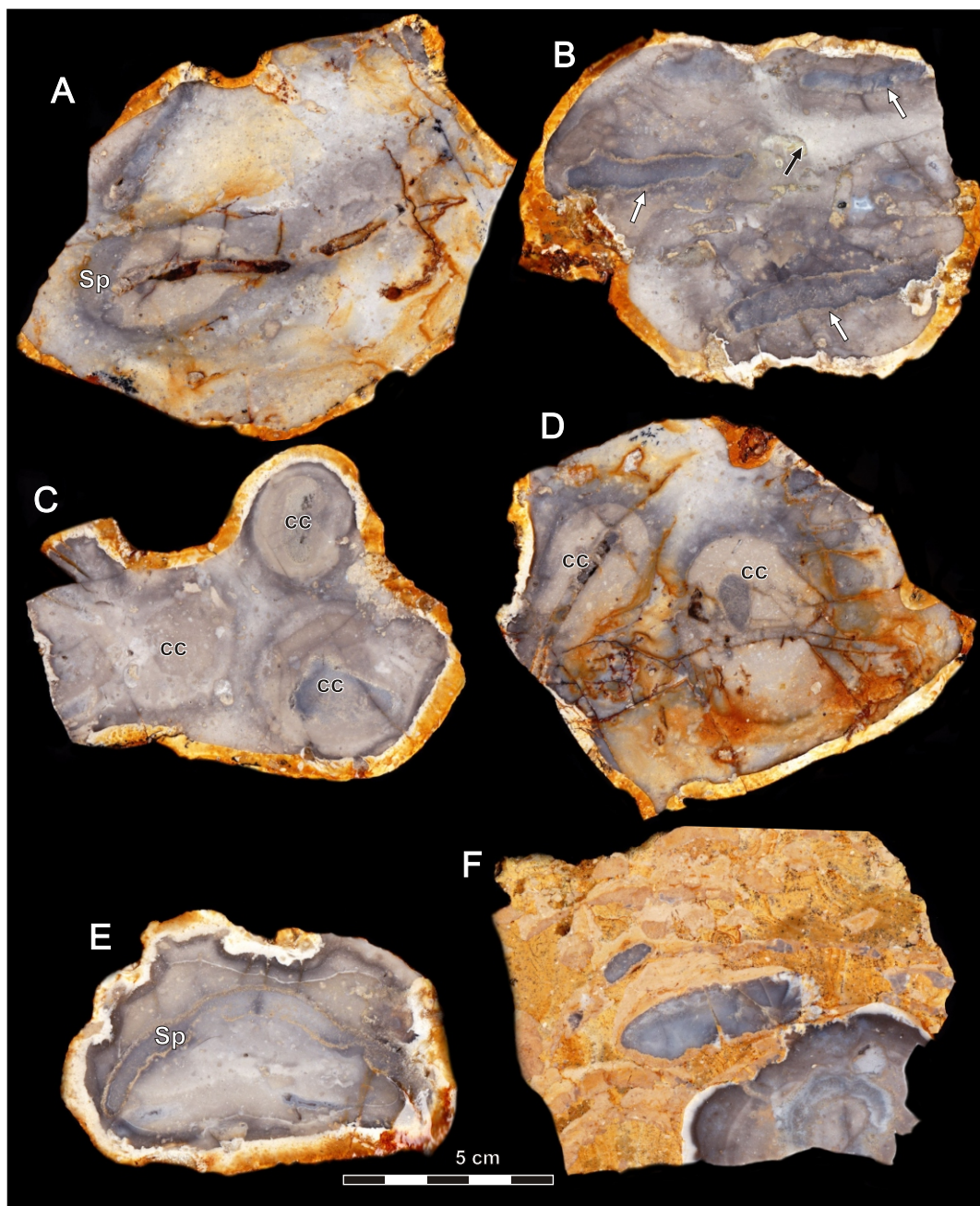


Fig. 11. Photographs of polished sections (Münster exposure)

A – core of chert concretion with bowl-shaped sponge cast (Sp). Some cracks are filled with brownish Fe-oxides. **B** – chert concretion of shape close to spherical with sponge casts, both flat (white arrows) and bowl-like (black arrow). **C** – irregularly shaped aggregate of 3 chert concretions (cc). **D** – fractured aggregate of 2 chert concretions (cc). Fractures are filled with brownish Fe-oxides. **E** – ellipsoidal chert concretion. The only recognizable component of its core is a cast of a siliceous sponge (Sp). **F** – three small chert concretions. Fragmentary cortex covers only a part of the largest concretion (at the bottom) whereas the remaining 2 smaller ones lack cortices

skeletons of siliceous sponges, tuberoïds, brachiopod and bivalve shells, serpulids, benthic foraminifers and *Crescientella* sp. Locally, numerous, scattered dolorhombes are present, particularly abundant at the contacts with stylolites filled with brownish Fe-oxides (Fig. 15A).

The first, macroscopically distinguished chert variety occurs in non- or poorly dolomitized limestones. Dark-grey cherts are composed of microcrystalline silica (Figs. 15B and 16A, B). Larger bioclasts are replaced by granular quartz or chalcedony

(Fig. 15B). Sporadically, one may encounter carbonate relics of bioclasts, mostly echinoderms as well as granular quartz infilling the larger, silicified bioclasts. The concretions and enclosing limestones contact along dissolution seams filled with brownish-rusty Fe-hydroxides. The latter are also observed as infillings of fractures cutting through the concretions (Fig. 15C, D). At the contact with enclosing limestones, cortices are usually about 2 mm thick with features that can be examined only in plane polarized light. Within the cortices, relics of partly silicified

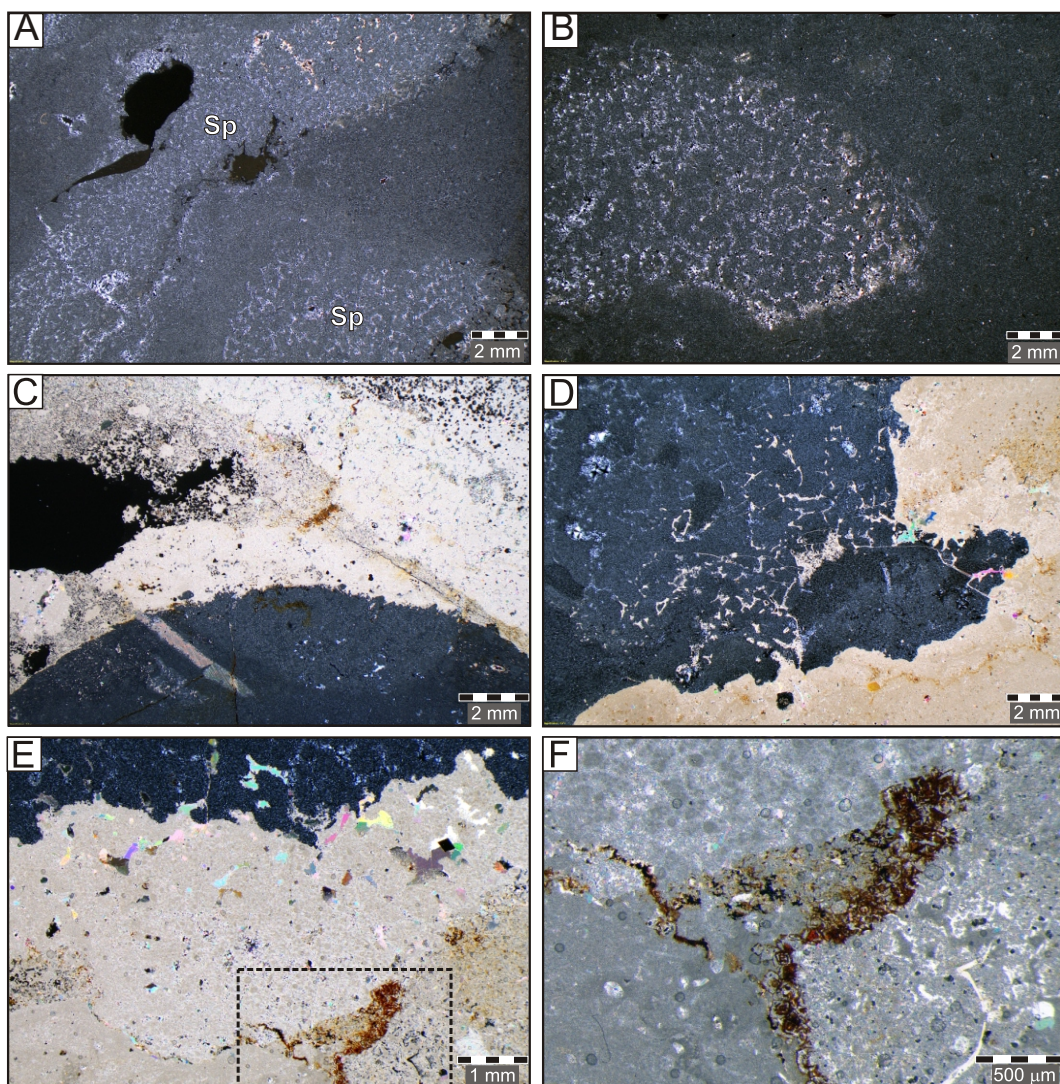


Fig. 12. Microfacies development of chert concretions and host limestones (Münster exposure)

A – chert concretion that originated from silicification of part of a unitary sedimentary sequence. The only identifiable components are skeletons of siliceous sponges (Sp). Crossed polars. **B** – skeleton of siliceous sponge in chert concretion. Crossed polars. **C** – contact of chert concretion (at the bottom) with partly dolomitized limestone. Dark spots in the upper right corner and in the centre-left, above an open space, are examples of mouldic porosity generated by dedolomitization. Crossed polars. **D** – contact of irregular chert concretion with partly dolomitized limestone. In the centre, skeletal fragments of siliceous sponge are filled with carbonate, which has not been secondary silicified. Crossed polars. **E** – contact of chert concretions with limestone containing dolorhombs. Area in rectangle is shown in Figure F. Crossed polars. **F** – stylolite cutting through limestone with euhedral dolorhombs. Some dolorhombs are dedolomitized and filled with Fe-oxides. Plane polarized light

limestones are present. In the central parts of concretions, primary textures of the silicified limestones are visible in plane polarized light, as “*pseudonodules*” and pressure solution features (Fig. 16A, B).

The second macroscopically identified concretion variety occurs in dolomitized limestones. This is completely silicified dolomite cross-cut by stylolites infilled with Fe-oxides (Fig. 16C, D).

Interpretation of depositional and diagenetic environments

The biostromal limestones from that sampling site are typical sediments of microbial-sponge megafacies. Two stages of dolomitization are suggested: (1) an early stage manifested by scattered dolorhombs and (2) a late stage related to chemical compaction and pressure solution. Silicification took place after both the dolomitization and pressure solution events.

CONCISE CHARACTERIZATION OF CHERT CONCRETIONS AND BEDDED CHERTS FROM UPPER JURASSIC STRATA OF THE KRAKÓW-CZĘSTOCHOWA UPLAND

Detailed characterization of chert concretions from the KCU can be found in a number of publications, e.g.: Matyszkiewicz et al. (2015), Kochman et al. (2020a, b), Krzyżak et al. (2020), Matyszkiewicz and Kochman (2020), Kochman and Matyszkiewicz (2023), and Fajt et al. (2024).

In the KCU, chert concretions are commonly encountered in Middle/Upper Oxfordian biostromal bedded limestones where these form horizons usually arranged parallel to the bedding surfaces. “Classic” exposures are located mostly in the S-KCU and were comprehensively described by e.g.: Dżułyński (1952),



Fig. 13. Flintsbach Quarry

- A** – part of abandoned quarry where poorly bedded limestones host single, randomly distributed chert concretions; **B** – greyish-white, spotted chert concretion located close to interbedding space; **C** – strongly fractured, light-cream chert concretion with cherry-red outer surface

Alexandrowicz (1955), Rajchel (1971), Matyszkiewicz (1989), Kochman et al. (2020a), Matyszkiewicz and Kochman (2020) and Kochman and Matyszkiewicz (2023). The shapes of chert concretions are ellipsoidal, spherical or irregular and may have diameters up to even some tens of centimetres (Fig. 17A, B, D–F). Colours of concretions are also diverse: grey, brownish or brownish-cherry with various shades and with irregular spots.

The "classic" chert concretions are silicified remains of biostromal limestones representing a microbial-sponge megafacies. Commonly, polished (Fig. 17B) and thin (Fig. 18B) sections reveal the presence of silicified unitary sedimentary sequences (cf. Gaillard, 1983; Matyszkiewicz, 1989) with identifiable skeletons of siliceous sponges (Fig. 17A, B, D–F) separated by fine-detrital wackestones (Fig. 18A). Dolomitization of limestones is rarely observed in the topmost part of the preserved Oxfordian/Kimmeridgian succession (Fig. 18D; Łaptaś, 1974; Krajewski and Olchowy, 2021).

The bedded cherts were described in detail by Matyszkiewicz (1996), Kochman et al. (2020a); Krzyżak et al. (2020); Matyszkiewicz and Kochman (2020) and Fajt et al. (2024). The cherts are hosted in calciturbidite sequences deposited around the Oxfordian/Kimmeridgian boundary. Their maximum thick-

ness reaches ~20 cm and their length along strike exceeds 5 m. Colours change from light-grey to dark-brownish. Macroscopically visible, subtle lamination is locally disturbed by spotty burrows developed immediately after deposition but prior to silicification (Fig. 17C). Within the silicified limestone beds, ellipsoidal chert concretions can be observed, several centimetres in diameter, which document the multistage nature of the silicification processes.

The bedded cherts represent selectively silicified successions of well-sorted calciturbidites, which is particularly evident under the microscope together with occasionally observed graded bedding (Fig. 18C).

DISCUSSION

Development of both the chert concretions and the bedded cherts is closely related to the lithology of the Upper Jurassic limestones that were silicified. The development of microbial-sponge megafacies was similar in the FA, BW and KCU regions

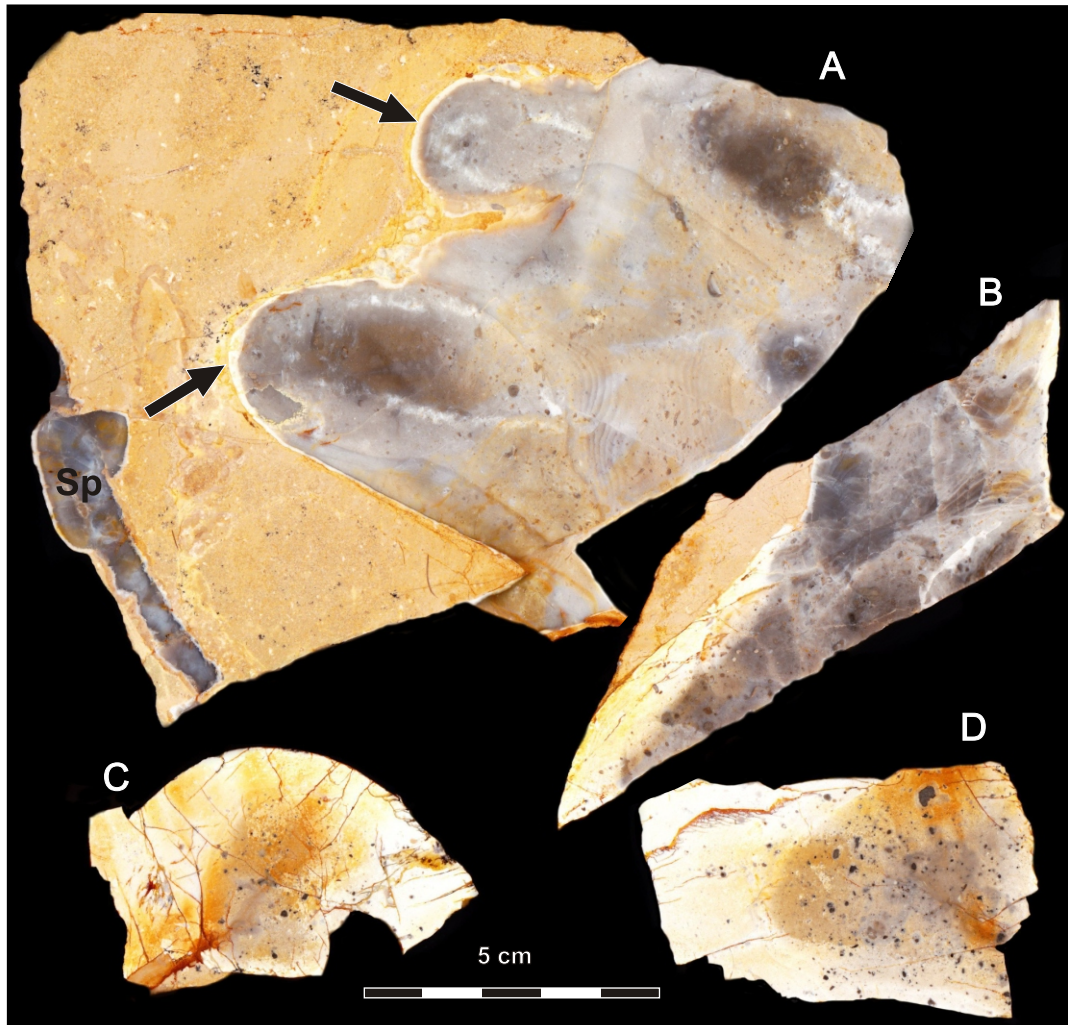


Fig. 14. Polished sections of chert concretions (Flintsbach Quarry)

A – on the right: an irregular aggregate of several chert concretions with only locally developed, thin cortex (arrows); on the left: silicified cast of siliceous sponge (Sp). Numerous white spots in the limestone, several millimetres in size, are *Crescientella* sp. **B** – spotted chert concretion. In the extreme left part, spots disappear and concretion colour changes to white-cream. **C, D** – parts of light-cream, strongly fractured concretions with dark spots representing accumulations of Fe-oxides

compared. This is particularly true for bedded biostromal limestones from around the Middle Oxfordian/Lower Kimmeridgian boundary, preserved in both the BW and KCU.

The most common type of chert concretions hosted in limestones from the BW and the KCU are silicified remains of microbial-sponge biostromes with a unitary sedimentary sequence pattern. Such chert concretions reveal far-reaching similarities in size, texture and colour (cf. Figs. 11, 12A, B, 14A, 17A, B, D–F and 18A, B). However, we consider that no premises have yet emerged that would allow the unambiguous identification of the site from which a particular chert concretion originates. Consequently, no premises exist which would allow distinguishing the JFAK as a separate category in siliceous artifacts inventories, which include specimens said too have been derived from the BW and the KCU.

We note that chert concretions from the BW, which do not have equivalents in the KCU, are very rare. This is true for concretions formed by silicification of pseudonodular limestones (Fig. 16A, B). Although such limestones, full of siliceous spon-

ges, are known from the KCU, these do not host chert concretions (Matyszkiewicz and Kochman, 2016). Another type of chert concretion, which occurs exclusively in the BW, is the product of silicification of already dolomitized limestones subjected to chemical compaction (Fig. 16C, D). In the KCU, partly dolomitized limestones are only sporadically observed (Łaptaś, 1974; Krajewski and Olchow, 2021) and chert concretions hosted in such deposits have not yet been encountered.

In the Upper Jurassic rocks from the FA, representing the Middle Kimmeridgian-Lower Tithonian stratigraphic interval, an increase is observed of both the amounts and diversity of fossil assemblages, particularly of shallow-marine fauna. Although strata of that age interval have not been preserved in the KCU, some chert concretions and tabular cherts from the FA are morphologically similar to deposits from around the Oxfordian/Kimmeridgian boundary in the KCU. This is true for tabular cherts originated from silicification of tempestites (Figs. 6A, 7A, 17C and 18C), which show many features in common with the bedded cherts from the KCU produced by silicification of calci-

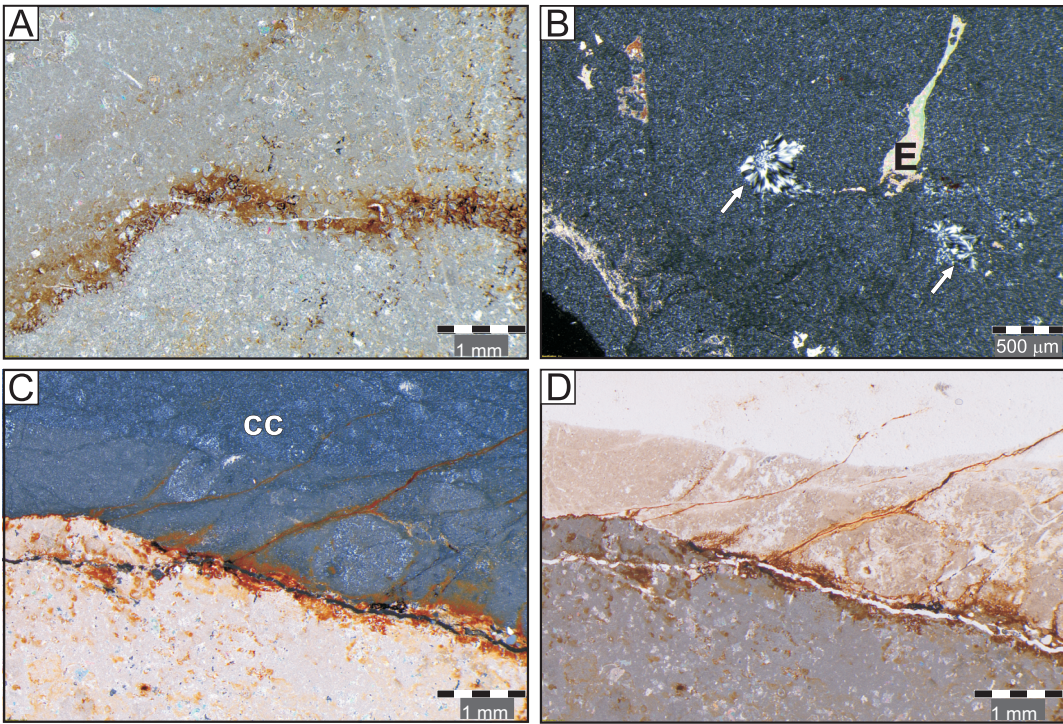


Fig. 15. Microfacies development of chert concretions and limestones (Flintsbach Quarry)

A – numerous dolomite crystals and brownish Fe-oxides located along stylolites cutting through the limestone. Plane polarized light. **B** – accumulations of chalcedony in chert concretion (arrows). Locally visible are non-silicified relics of carbonate bioclasts, mostly echinoderms (E). **C** – contact of chert concretion (cc) and limestone which contains euhedral dolomite crystals. Rusty Fe-oxides are accumulated along this contact and fill the fractures cutting through the concretion. Crossed polars. **D** – area of Figure C seen in plane polarized light. In the peripheral part of that concretion, a band of only partly silicified cortex is visible

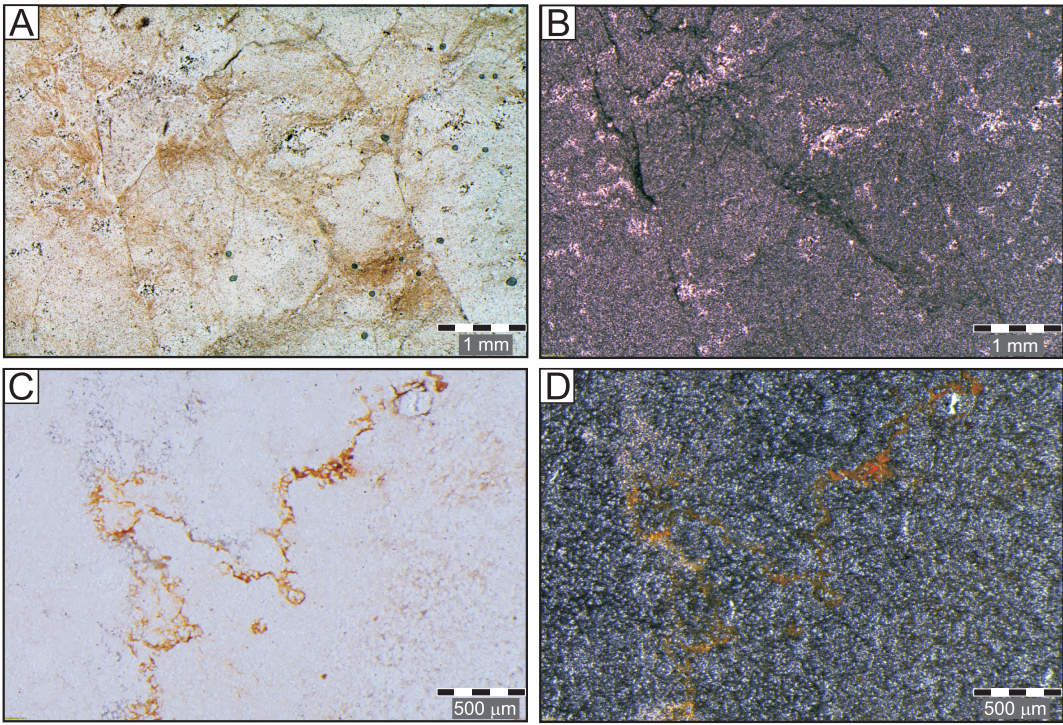


Fig. 16. Microfacies development of chert concretions (Flintsbach Quarry)

A – primary texture of pseudonodular limestone preserved in chert concretion. Pseudonodules contact each other along dissolution seams and stylolites. Plane polarized light. **B** – area shown in Figure A under crossed polars. **C** – silicified dolomite with stylolites locally filled with Fe-oxides. Plane polarized light. **D** – area shown in Figure C under crossed polars

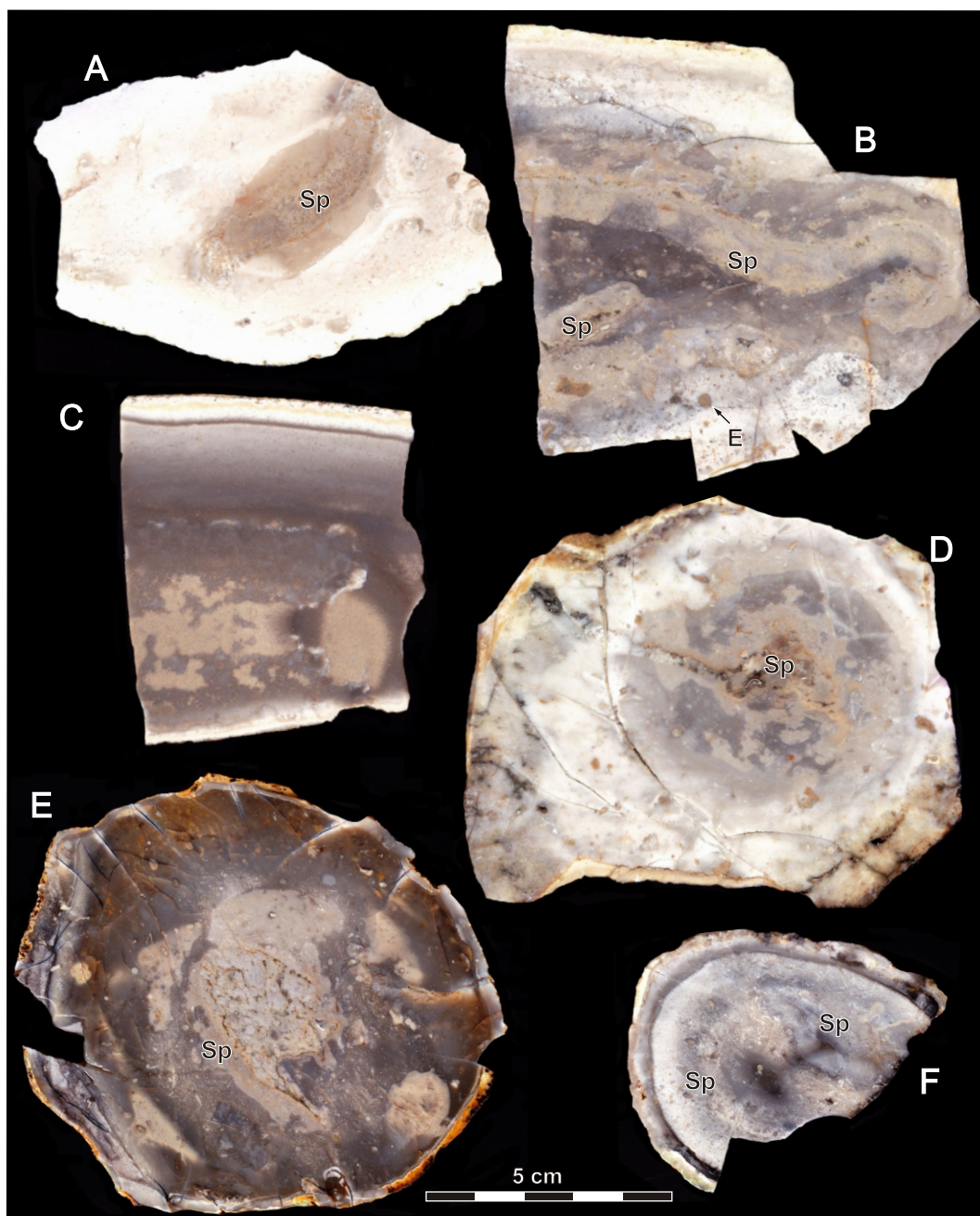


Fig. 17. Photographs of selected polished sections of chert concretions and bedded cherts from Upper Jurassic limestones showing macroscopic similarities to strata of the Franconian Alb and the Bayerwald (Kraków-Częstochowa Upland)

A – chert concretion with sponge cast in the centre (Sp). Towards the edges, the colour of concretion becomes increasingly lighter. Exposure in Siedlec near Częstochowa (cf. Fig. 3C). **B** – chert concretion with spotted core which contains casts of siliceous sponges (Sp), echinoid spines (E) and fine, unrecognizable bioclasts. Guminek Hill in Kraków (cf. Figs. 6E and 9E). **C** – bedded chert with flat upper and bottom surfaces. Spotted structure is related to burrows in carbonate sediment that was then subjected to silicification. Wielkanoc Hill in Kraków (cf. Fig. 6A). **D–F** – close-to-spherical chert concretions with bowl-shaped casts of sponges (Sp) in the centre. Guminek, Wielkanoc and Bodzów hills in Kraków (cf. Fig. 11)

turbidites (Matyszkiewicz, 1996) as well as with the chert concretions developed as silicified patches of biostromal limestones containing skeletons of siliceous sponges (Figs. 3C, D and 9E, F).

Determination of the provenance of siliceous artifacts based upon colour can be questionable, as demonstrated by the specific development of a chert concretion collected from the Kelheim exposure (Figs. 6D and 7D). In that specimen, one part is grey and another part is brownish, the latter being similar to

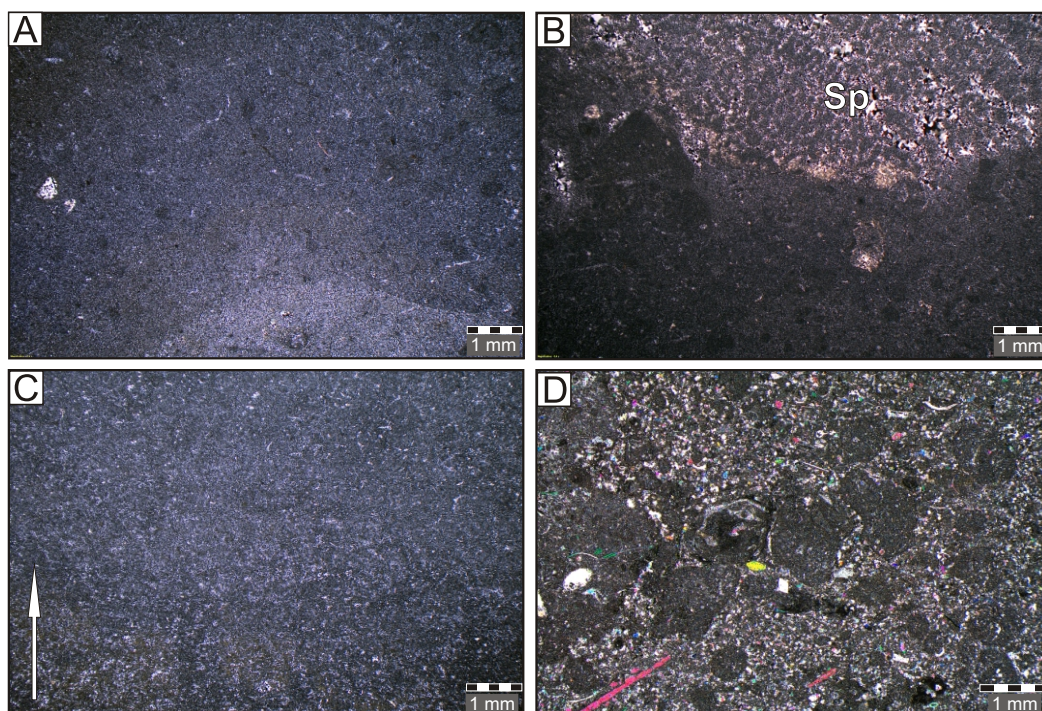


Fig. 18. Photographs of selected polished sections of chert concretions and bedded cherts from Upper Jurassic limestones showing macroscopic similarities to strata of the Franconian Alb and the Bayerwald (Kraków-Częstochowa Upland)

A – chert concretion developed as a silicified wackestone. Crossed polars. Exposure in Siedlec near Częstochowa (cf. Figs. 3D and 12A, B). **B** – chert concretion with preserved siliceous sponge skeleton (Sp). Crossed polars. Guminek Hill in Kraków (cf. Figs. 3D and 12A, B). **C** – bedded chert developed as perfectly sorted detritus of *Saccocoma* sp. and micropeloids of similar diameters. Arrow indicates direction to the top. Crossed polars. Wielkanoc Hill in Kraków (cf. Fig. 7A). **D** – dolomitized limestone with detritus of echinoderms and numerous, irregular, non-dolomitized oncoids. Euhedral dolomite crystals are present only in the matrix. Plane polarized light. Exposure in Kurdwanów residential district, in Kraków (cf. Fig. 3F)

the typical CF of Poland. The brownish part of that concretion may provide sufficient raw material for at least several tools even larger than the artifacts described by Burgert (2018: p. 56), who identified their source as the CF based only on colour. Moreover, Burgert (2018) cited 22 archaeological sites from Bohemia where siliceous artifacts were found, and concluded that their source raw material was from the CF. Surprisingly, in 11 of these sites, the CF was alleged as the source raw material based solely on a single artifact or on 3 such artifacts found in each of 5 other sites. In our opinion, the identification of CF in archaeological inventories based upon single artifacts may well be erroneous.

CONCLUSIONS

The results of petrographic observations of chert concretions and bedded cherts from the southeastern Franconian Alb and the Bayerwald point out to late-diagenetic, multistage silicification, indicated by:

- a silicified pseudonodular texture resulting from chemical compaction (Fig. 16A, B);
- boundaries of chert concretions developed on stylolites resulted from pressure solution (Fig. 4C, D);

– silicification of convoluted, dolomitized and dedolomitized laminae (Fig. 9C, D).

Moreover, the ^{57}Fe Mössbauer spectral analysis documents the multistage character of silicification and diverse sources of silica. This evidence allows rejection of the widespread opinion that the silica was sourced from the dissolution of skeletons of siliceous sponges. Presumably, the main sources of silica were local hydrothermal processes, as proposed by Migaszewski et al. (2006, 2022), Matyszkiewicz et al. (2015, 2016), Kochman et al. (2020a) and Kochman and Matyszkiewicz (2023).

Although observations of polished and thin-sections may occasionally disclose petrographic features providing some indications of the provenance of fresh chert concretions and bedded cherts, this is highly unlikely in the case of the uneven and weathered surfaces of siliceous artifacts. Taking into account that such artifacts were usually manufactured from the inner parts of chert concretions or bedded cherts, from which the enclosing limestones were intentionally removed during the processing in workshops, identification of the provenance of such artifacts based upon colour may well lead to erroneous conclusions.

Acknowledgements. The authors gratefully acknowledge A. Błachowski (AGH University of Krakow, Faculty of Geology, Geophysics and Environmental Protection) for performing the

Mössbauer measurement. Sincere thanks are due to A. Górny for assistance in the fieldwork and inspiring discussions. We benefited greatly from the perceptive comments and suggestions of A. Muszyński and an anonymous reviewer.

These studies were carried out within the framework of the "Processes controlling the formation of chert nodules and

bedded cherts in the Upper Jurassic sediments from the Kraków-Częstochowa Upland" grant which was funded by the National Science Centre, Poland, contract no. UMO-2017/27/B/ST10/00594 for the period 2018-2021.

REFERENCES

- Alexandrowicz, S.W., 1955.** Notes on the origin of the Vistula Gap at Tyniec (near Cracow) (in Polish with English summary). *Biuletyn Instytutu Geologicznego*, **97**: 271–295.
- Bertola, S., Schäfer, D., 2013.** Silex raw materials from the Kelheim district (Bavaria, Germany) in the lithic assemblage of the Lower Mesolithic site Ullafelsen (Tyrolean Alps, Austria). *Erlangen Studien zur Prähistorischen Archäologie*, **1**: 59–69.
- Binstener, A., 2001.** Die Feuersteinstraße zwischen Bayern und Böhmen. Eine Studie zur Verbreitung der Arnhoferer und Baidersdorfer Jurahornsteine. *Bayerische Vorgeschichtsblätter*, **66**: 7–12.
- Binstener, A., 2005.** Die Lagerstätten und der Abbau Bayerischer Jurahornstein sowie deren Distribution im Neolithikum Mittel- und Osteuropas. *Jahrbuch des Römisch-Germanischen Zentralmuseums*, **52**: 43–155.
- Binstener, A., 2013.** Die Silexartefakte aus dem Chamer Erdwerk von Riekofen (Lkr. Regensburg). *Archäologisches Korrespondenzblatt*, **43**: 19–28.
- Błachowski, A., Reubenbauer, K., Żurkowski, J., Górnicki, R., 2008.** Early design stage of the MsAa-4 Mössbauer Spectrometer. *Acta Physica Polonica A*, **114**: 1707–1713.
- Brachert, T.C., 1992.** Sequence stratigraphy and paleo-oceanography of an open-marine mixed carbonate/siliciclastic succession (Late Jurassic, Southern Germany). *Facies*, **27**: 191–216; <https://doi.org/10.1007/BF02536812>
- Brandl, M., Hauzenberger, C., Martinec, M.M., Filzmoser, P., Werra, D.H., 2016.** The application of the multi-layered chert sourcing approach (MLA) for the characterisation and differentiation of 'Chocolate Silicites' from the Holy Cross Mountains, South-Central Poland. *Archaeologia Austriaca*, **100**: 119–149; <https://doi.org/10.1553/archaeologia100s119>
- Budziszewski, J., 2008.** Stan badań nad występowaniem i prądziejową eksploatacją krzemieni czekoladowych (in Polish). In: *Krzemień czekoladowy w prądziejach. Materiały z konferencji w Orońsku, 08–10.10.2003. Studia nad gospodarką surowcami krzemiennymi w prądziejach 7* (eds. W. Borkowski, J. Libera, B. Sałacińska and S. Sałaciński): 33–106. Instytut Archeologii UMCS and Państwowe Muzeum Archeologiczne, Warszawa–Lublin.
- Burgert, P., 2016.** Bavarian Jurassic chert of the Franconian Jura in the Bohemian Neolithic and Eneolithic (in Czech with English summary). *Archeologické rozhledy*, **68**: 91–108.
- Burgert, P., 2018.** The status and the role of "Chocolate" silicite in the Bohemian Neolithic. *Archaeologia Polona*, **56**: 49–64; <https://doi.org/10.23858/APA56.2018.004>
- Chatzimpaloglou, P., French, C., Pedley, M., Stoddart, S., 2020.** Connecting chert sources of Sicily with Neolithic chert artefacts of Malta. *Journal of Archaeological Science: Reports*, **29**, 102111; <https://doi.org/10.1016/j.jasrep.2019.102111>
- Chochorowska, E., Dagnan-Ginter, A., 1995.** Najstarsze ślady pobytu człowieka na Jurze Krakowskiej (starsza i środkowa epoka kamienia) (in Polish). In: *Pradzieje i średniowiecze. Natura i kultura w krajobrazie Jury Tom IV*: 15–48. Zarząd Zespołu Jurajskich Parków Krajobrazowych w Krakowie, Kraków.
- Čuláková, K., 2015.** Příspěvek k poznání mezolitického osídlení Čech (in Czech). Ph.D. Thesis, Charles University in Prague.
- Dagnan-Ginter, A., Drobniewicz, B., Ginter, B., Sobczyk, K., 1976.** Brzostkwinia-Krzemionki, province of Krakow (the group of Palaeolithic sites). *Recherches Archeologiques de 1975*: 5–10.
- Doben, K., Doppler, G., Freudenberger, W., Jerz, H., Meyer, R.K.F., Mielke, H., Ott, W.D., Rohrmüller, J., Schmidt-Kaler, H., Schwerd, K., Unger, H.J., 1996.** Geologische Karte von Bayern 1:500 000. Bayerisches Geologisches Landesamt, Augsburg.
- Dunham, R.J., 1962.** Classification of carbonate rocks according to depositional texture. *AAPG Memoir*, **1**: 108–121; <https://doi.org/10.1306/M1357>
- Dzieduszycka-Machnikowa, A., Lech, J., 1976.** Neolityczne zespoły pracowniane z kopalni krzemienia w Sępowie (in Polish). *Polskie Badania Archeologiczne*, **19**: 1–171.
- Dzudyński, S., 1952.** The origin of the Upper Jurassic limestones in the Cracow area (in Polish with English summary). *Rocznik Polskiego Towarzystwa Geologicznego*, **21**: 125–180.
- Engelhardt, B., 1985.** Das neolithische Silexbergwerk von Arnhofen. *Das Archäologische Jahr in Bayern 1984*: 35–36.
- Fajt, M., Mazur-Rozmus, W., Stefańska, A., Kochman, A., Krzyżak, A.T., 2024.** Chert outcrops differentiation by means of low-field NMR relaxometry. *Scientific Reports*, **14**, 25280; <https://doi.org/10.1038/s41598-024-75945-6>
- Freyberg, B. v., 1964.** Geologie des Weißen Jura zwischen Eichstätt und Neuburg/Donau (Südliche Frankenalb). *Erlanger Geologische Abhandlungen*, **54**: 1–97.
- Freyberg, B. v., 1968.** Übersicht über den Malm der Altmühl-Alb. *Erlanger Geologische Abhandlungen*, **70**: 1–40.
- Gaillard, C., 1983.** Les biohermes à spongiaires et leur environnement dans l'Oxfordian du Jura méridional. *Documents des Laboratoires de Géologie de la Faculté des Sciences de Lyon*, **90**: 1–515.
- Ginter, B., 1980.** Brzostkwinia, "Krzemionki" woj. Kraków. In: *5000 Jahre Feuersteinbergbau. Die Suche nach dem Stahl der Steinzeit* (eds. G. Weisgerber, R. Slotta and J. Weiner): 624–626. Bergbau-Museum Bochum, Bochum.
- Grooth, M.E.Th. de, 1994.** Chert procurement strategies in the LBK settlement of Meindling, Bavaria. *Analecta Praehistorica Leidensina*, **25**: 43–53.
- Grooth, M.E.Th. de, 1995.** The organization of chert exploitation in Southeastern Bavaria during the Neolithic. *Archaeologia Polona*, **33**: 163–172.
- Grooth, M.E.Th. de, 1997.** Social and economic interpretations of the chert procurement strategies of the Bandkeramik settlement at Hienheim, Bavaria. *Analecta Praehistorica Leidensina*, **29**: 91–98.
- Gröschke, M., 1985.** Stratigraphie und Ammonitenfauna der Jurarelikte zwischen Straubing und Passau (Niederbayern). *Palaeontographica, Abteilung A*, **191**: 1–68.

- Gwinner, M.P., 1971.** Carbonate rocks of the Upper Jurassic in SW-Germany. In: *Sedimentology of Parts of Central Europe* (ed. G. Müller): 193–207. Kramer, Frankfurt a. M.
- Gwinner, M.P., 1976.** Origin of the Upper Jurassic Limestones of the Swabian Alb (Southern Germany). *Sedimentary Geology*, **5**: 1–76.
- Janák, V., Přichystal, A., 2007.** Distribution of silicites of the Kraków-Częstochowa Jurassic in Moravia and Upper Silesia in the Neolithic and at the beginning of the Eneolithic (in Czech with English summary). *Památky archeologické*, **98**: 5–30.
- Kaczanowska, M., Kozłowski, J.K., 1976.** Studia nad surowcami krzemieniami południowo-wschodniej części Wyżyny Krakowsko-Częstochowskiej (in Polish). *Acta Archaeologica Carpathica*, **16**: 201–216.
- Keupp, H., Koch, R., Leinfelder, R., 1990.** Steuerungsprozesse der Entwicklung von Oberjura-Spongiolithen Süddeutschlands: Kenntnisstand, Probleme und Perspektiven. *Facies*, **23**: 141–174; <https://doi.org/10.1007/BF02536711>
- Kleinschnitz, M., 2001.** Kurzerläuterung zur Geologischen Karte 1:25000 7134 Gaimersheim. Bayerisches Geologisches Landesamt, München.
- Kochman, A., Matyszkiewicz, J., 2023.** The development and origin of the two-stage silicification of Upper Jurassic limestones from the northern part of the Kraków-Częstochowa Upland (Southern Poland). *Geology, Geophysics and Environment*, **49**: 225–243; <https://doi.org/10.7494/geol.2023.49.3.225>
- Kochman, A., Matyszkiewicz, J., Wasilewski, M., 2020a.** Siliceous rocks from the southern part of the Kraków-Częstochowa Upland (Southern Poland) as potential raw materials in the manufacture of stone tools – a characterization and possibilities of identification. *Journal of Archaeological Science: Reports*, **30**, 102195; <https://doi.org/j.jasrep.2020.102195>
- Kochman, A., Kozłowski, A., Matyszkiewicz, J., 2020b.** Epigenetic siliceous rocks from the southern part of the Kraków-Częstochowa Upland (Southern Poland) and their relation to Upper Jurassic early diagenetic chert concretions. *Sedimentary Geology*, **401**, 105636; <https://doi.org/10.1016/j.sedgeo.2020.105636>
- Kozłowski, J.K., 1958.** Przyczynki do znajomości surowców krzemienistych występujących w paleolicie i neolicie Č.S.R. (in Polish). *Wiadomości Archeologiczne*, **25**: 355–360.
- Kowalski, S., Kozłowski, J.K., 1958.** Neolityczna pracownia krzemieniarska w miejscowości Bębło, pow. Olkusz (in Polish). *Wiadomości Archeologiczne*, **25**: 339–354.
- Krajcarz, M.T., Sudol-Procyk, M., 2019.** The mine of chocolate flint in the Udorka Valley (Kraków-Częstochowa Upland). *Field Trip Guide*. In: *UISPP Commission on Flint Mining in Pre- and Proto-historic Times „The Flint Mining Studies: Archaeological Excavations – Extraction Methods – Chipping Floors – Distribution of Raw Materials and Workshop Products”*, Field Guide, 19-21th (eds. D.H. Werra, M. Sudol-Procyk, A. Jedynak, K. Kaptur and M.T. Krajcarz): 33–37. Archeological Museum and Reserve „Krzemionki”, Ostrowiec Świętokrzyski.
- Krajcarz, M.T., Sudol, M., Krajcarz, M., Cyrek, K., 2012.** From far or from near? Sources of Kraków-Częstochowa banded and chocolate silicite raw material used during the Stone Age in Biśnik Cave (southern Poland). *Anthropologie*, **50**: 411–425.
- Krajewski, M., Olchowy, P., 2021.** Upper Jurassic bedded limestones and early diagenetic dolomitized limestones in the light of mineralogical, geochemical and sedimentological studies; Kraków Area, Poland. *Minerals*, **11**, 462; <https://doi.org/10.3390/min11050462>
- Krajewski, M., Olchowy, P., Rudziński, D., 2018.** Sedimentary successions in the Middle-Upper Oxfordian reef deposits from the southern part of the Kraków-Częstochowa Upland (Southern Poland). *Geological Quarterly*, **62**: 653–668; <https://doi.org/10.7306/gq.1429>
- Krukowski, S., 1920.** Pierwociny krzemieniarskie górnictwa, transportu i handlu w holocenie Polski (in Polish). *Wiadomości Archeologiczne*, **5**: 185–206.
- Krzyżak, A.T., Mazur, W., Matyszkiewicz, J., Kochman, A., 2020.** Identification of proton populations in cherts as natural analogues of pure silica materials by means of low field NMR. *Journal of Physical Chemistry C*, **124**: 5225–5240; <https://doi.org/10.1021/acs.jpcc.9b11790>
- Kutek, J., Wierzbowski, A., Bednarek, J., Matyja, B.A., Zapaśnik, T., 1977.** Notes on the Upper Jurassic stratigraphy in the Polish Jura Chain (in Polish with English summary). *Przegląd Geologiczny*, **25**: 438–445.
- Lech, J., 1980.** Geologia krzemienia jurajskiego-podkrakowskiego na tle innych skał krzemionkowych. Wprowadzenie do badań z perspektywy archeologicznej (in Polish). *Acta Archaeologica Carpathica*, **20**: 165–230.
- Lech, J., 1989.** A Danubian raw material exchange network: a case study from Byłany. In: *Byłany Seminar 1987* (ed. J. Rulf): 111–120. Collected Papers, Praha.
- Lech, J., 1993.** Analyse der Spaltindustrie aus der Grube 2. In: *Chrás any, Bez. Rakovník. Ein Beitrag zum chronologischen Verhältnis der Stichtbandkeramik zur Grossgartacher und Oberlauterbacher Keramik* (ed. M. Zápotocká), *Archeologické rozhledy*, **45**: 436–459.
- Luedtke, B., 1979.** The Identification of Sources of Chert Artifacts. *American Antiquity*, **44**: 744–757; <https://doi.org/10.2307/279116>
- Łaptaś, A., 1974.** The dolomites in the Upper Jurassic limestones in the area of Cracow (Southern Poland) (in Polish with English summary). *Rocznik Polskiego Towarzystwa Geologicznego*, **34**: 247–273.
- Mandera, S., Sudol-Procyk, M., Malak, M., Skrzatek, M., Krajcarz, M.T., 2024.** New deposit of chocolate flint in Załęże gully (Kraków-Częstochowa Upland, Poland) – raw material characterization and its availability for prehistoric communities. *Journal of Archaeological Science: Reports*, **53**, 104328; <https://doi.org/10.1016/j.jasrep.2023.104328>
- Mateiciucová, I., 2008.** Talking stones: the chipped Industry in Lower Austria and Moravia and the beginnings of the Neolithic in Central Europe (LBK), 5700–4900 BC. In: *Dissertationes Archaeologicae Brunenses/Pragensesque 4* (eds. Z. Měřínský and J. Klápště): 1–357. Masarykova University, Brno.
- Mateiciucová, I., Trnka, G., 2015.** Long-distance distribution of raw materials for chipped stone artefacts in the Neolithic of Central Europe (Moravia and eastern Austria) in the 6th and 5th millennia BC. In: *Connecting Networks: Characterising Contact by Measuring Lithic Exchange in the European Neolithic* (eds. T. Kerig and S. Shennan): 8–15. Archaeopress, Oxford.
- Matyszkiewicz, J., 1989.** Sedimentation and diagenesis of the Upper Oxfordian cyanobacterial-sponge limestones in Piekary near Kraków. *Annales Societatis Geologorum Poloniae*, **59**: 201–232.
- Matyszkiewicz, J., 1996.** The Significance of Saccocoma-calciturbidites for the analysis of the Polish Epicontinental Late Jurassic Basin: an example from the Southern Cracow-Wieluń Upland (Poland). *Facies*, **34**: 23–40; <https://doi.org/10.1007/BF02546155>
- Matyszkiewicz, J., 1997.** Microfacies, sedimentation and some aspects of diagenesis of Upper Jurassic sediments from the elevated part of the Northern peri-Tethyan Shelf: a comparative study on the Lothen area (Schwäbische Alb) and the Cracow area (Cracow-Wieluń Upland, Polen). *Berliner Geowissenschaftliche Abhandlungen*, **E21**: 1–111.
- Matyszkiewicz, J., 1999.** Sea-bottom relief versus differential compaction in ancient platform carbonates: a critical reassessment of an example from Upper Jurassic of the Cracow-Wieluń Upland. *Annales Societatis Geologorum Poloniae*, **69**: 63–79.
- Matyszkiewicz, J., Kochman, A., 2016.** Pressure dissolution features in Oxfordian microbial-sponge buildups with pseudonodular texture, Kraków Upland. *Annales Societatis Geologorum Poloniae*, **86**: 355–377; <https://doi.org/10.14241/asgp.2016.008>
- Matyszkiewicz, J., Kochman, A., 2020.** The provenance of siliceous rocks from the Kraków-Częstochowa Upland (Poland) used as raw-materials in the manufacture of siliceous artefacts from Central-Eastern Europe; an old problem in new light. *Journal of Archaeological Science: Reports*, **34**, Part A, 102600; <https://doi.org/10.1016/j.jasrep.2020.102600>

- Matyszkiewicz, J., Kochman, A., Rzepa, G., Gołębiowska, B., Krajewski, M., Gaidzik, K., Żaba, J., 2015. Epigenetic silicification of the Upper Oxfordian limestones in the Sokole Hills (Kraków-Częstochowa Upland): relationship to facies development and tectonics. *Acta Geologica Polonica*, **65**: 181–203; <https://doi.org/10.1515/agp-2015-0007>
- Matyszkiewicz, J., Krajewski, M., Kochman, A., Kozłowski, A., Duliński, M., 2016. Oxfordian neptunian dykes with brachiopods from the southern part of the Kraków-Częstochowa Upland (Southern Poland) and their links to hydrothermal vents. *Facies*, **62**, 12; <https://doi.org/10.1007/s10347-016-0464-x>
- Meischner, K.D., 1964. Alldapische Kalke, Turbidite in Riff-Nahen Sedimentations-Becken. *Developments in Sedimentology*, **3**: 156–191; [https://doi.org/10.1016/S0070-4571\(08\)70963-4](https://doi.org/10.1016/S0070-4571(08)70963-4)
- Meyer, R.K.F., 1975. Mikrofazielle Untersuchungen in Schwamm-Biohermen und -Biostromen des Malm Epsilon (Ober-Kimmeridge) und obersten Malm Delta der Frankenalb. *Geologische Blätter für Nordost-Bayern*, **25**: 149–177.
- Meyer, R.K.F., 1977. Stratigraphie und Fazies des Frankendolomits und der Massenkalk (Malm), 3. Teil: Südliche Frankenalb. *Erlanger Geologische Abhandlungen*, **104**: 1–41.
- Meyer, R.K.F., 2003a. Kurzerläuterung zur Geologischen Karte 1:25000 7035 Schamhaupten. Bayerisches Geologisches Landesamt, München.
- Meyer, R.K.F., 2003b. Kurzerläuterung zur Geologischen Karte 1:25000 7135 Kösching. Bayerisches Geologisches Landesamt, München.
- Meyer, R.K.F., 2003c. Kurzerläuterung zur Geologischen Karte 1:25000 7033 Titting. Bayerisches Geologisches Landesamt, München.
- Meyer, R.K.F., Schmidt-Kaler, H., 1990. Paläogeographie und Schwammriffentwicklung des süddeutschen Malm – ein Überblick. *Facies*, **23**: 175–184; <https://doi.org/10.1007/BF02536712>
- Migaszwski, Z.M., Gałuszka, A., Durakiewicz, T., Starnawska, E., 2006. Middle Oxfordian – Lower Kimmeridgian chert nodules in the Holy Cross Mountains, south-central Poland. *Sedimentary Geology*, **187**: 11–28; <https://doi.org/10.1016/j.sedgeo.2005.12.003>
- Migaszwski, Z.M., Gałuszka, A., Migaszwski, A., 2022. Geochemistry and petrology of striped chert as a provenance tool for artefacts from the Krzemionki neolithic mining area (Poland). *Archaeometry*, **64**: 1093–1109; <https://doi.org/10.1111/arcim.12778>
- Nerudová, Z., Přichystal, A., 2011. Kamenná štípaná industrie (in Czech). In: *Osídlení kultury s lineární keramikou v Kosofě, okr. Praha-západ* (ed. M. Lička): 78–86. *Fontes Archaeologici Pragenses* 37. Národní muzeum v Praze, Praha.
- Niebuhr, B., 2014. Lithostratigraphie der mittel- bis oberjurasischen Reliktorkommen zwischen Straubing und Passau (Niederbayern). *Schriftenreihe der Deutschen Gesellschaft für Geowissenschaften*, **83**: 73–82.
- Niebuhr, B., Pürner, T., 2014. Plattenkalk und Frankendolomit – Lithostratigraphie der Weißjura-Gruppe der Frankenalb (außer-alpiner Oberjura, Bayern). *Schriftenreihe der Deutschen Gesellschaft für Geowissenschaften*, **83**: 5–72.
- Oliva, M., 2001. Gravettianská sídliště u Pavlova. K otázce využívání silicítů krakovské jury (in Czech). *Acta Musei Moraviae, Scientiae sociales*, **86**: 45–99.
- Oliva, M., 2007. Gravettien na Moravě (in Czech). *Dissertationes archaeologicae Brunenses/Pragensesque*, 1, Masarykova Univerzita, Brno.
- Parish, R.M., 2011. The application of visible/near-infrared reflectance (VNIR) spectroscopy to chert: a case study from the Dover Quarry sites, Tennessee. *Geoarchaeology*, **26**: 420–439; <https://doi.org/10.1002/gea.20354>
- Pleslová-Štiková, E., 1969. Die Beziehungen zwischen Bayern und Westböhmen im Äneolithikum. *Bayerische Vorgeschichtsblätter*, **34**: 1–29.
- Přichystal, A., 1985. Chipped industry from the Neolithic site at Bylany (distr. Kutná Hora) from the point of view of the applied raw materials and of their origin. *Archeologické rozhledy*, **37**: 481–488.
- Přichystal, A., 2013. *Lithic Raw Materials in Prehistoric Times of Eastern Central Europe*. Masaryk University, Brno.
- Přichystal, A., 2018. Artefacts Made from Siliceous Rocks of Polish Origin on Prehistoric Sites in the Czech Republic. *Archaeologia Polona*, **56**: 35–48; <https://doi.org/10.23858/APa56.2018.003>
- Přichystal, A., Šebela, L., 2009. A contribution towards the stone industry from the Bell Beaker cemetery at Prague-Velká Chuchle (in Czech with English summary). *Archeologie ve středních Čechách*, **13**: 683–686.
- Rajchel, J.M., 1971. Badania sedymentologiczne krzemieni jurajskich pod Krakowem (in Polish). *Sprawozdania z Posiedzeń Komisji Naukowych Polskiej Akademii Nauk. Oddział w Krakowie*, **14**: 625–645.
- Reisch, L., 1974. Der vorgeschichtliche Hornsteinabbau bei Lengfeld, Ldkr. Kelheim und die Interpretation „grobgerätiger“ Silexindustrien in Bayern. *Materialhefte zur Bayerischen Vorgeschichte* 29. Kallmünz/ Opf.: Verlag Michael Lassleben.
- Roll, T.E., Neeley, M., Speakman, R.J., Glascock, M.D., 2005. Characterization of Montana cherts by LA-ICP-MS. In: *Laser Ablation-ICP-MS in Archaeological Research* (eds. R.J. Speakman and H. Neff): 58–76. University of New Mexico Press, Albuquerque.
- Rutte, E., 1962. Geologische Karte mit Erläuterung 1:25000 7037 Kelheim. Bayerisches Geologisches Landesamt, München.
- Rühle, E., Ciuk, E., Osika, R., Znosko, J., 1977. Mapa geologiczna Polski bez utworów czwartorzędowych: 1:500 000 (in Polish). Wydaw. Geol., Warszawa.
- Sánchez de la Torre, M., Le Bourdonnec, F.X., Gratuze, B., Domingo, R., García-Simón, L.M., Montes, L., Mazo, C., Utrilla, P., 2017. Applying ED-XRF and LA-ICP-MS to geochemically characterize chert. The case of the Central-Eastern Pre-Pyrenean lacustrine cherts and their presence in the Magdalenian of NE Iberia. *Journal of Archaeological Science: Reports*, **13**: 88–98; <https://doi.org/10.1016/j.jasrep.2017.03.037>
- Schild, R., 1971. Location of the so-called chocolate flint extraction sites on the north-eastern footslopes of the Holy Cross Mountains. *Folia Quaternaria*, **39**: 1–61.
- Schürch, B., Wettengl, S., Fröhle, S., Conard, N., Schmidt, P., 2022. The origin of chert in the Aurignacian of Vogelherd Cave investigated by infrared spectroscopy. *PLoS ONE*, **17**, e0272988; <https://doi.org/10.1371/journal.pone.0272988>
- Skarpelis, N., Carter, T., Contreras, D.A., Mihailović, D.D., 2017. Characterization of the siliceous rocks at Stélida, an early prehistoric lithic quarry (Northwest Naxos, Greece), by petrography and geochemistry: a first step towards chert sourcing. *Journal of Archaeological Science: Reports*, **12**: 819–833; <https://doi.org/10.1016/j.jasrep.2016.11.015>
- Sobczyk, K., 1993. The Late Palaeolithic Flint Workshops at Brzozkwinia-Krzemionki near Kraków. *Uniwersytet Jagielloński, Kraków*.
- Streim, W., 1961. Stratigraphie, Fazies und Lagerungsverhältnisse des Malms bei Dietfurt und Hemau (Südliche Frankenalb). *Erlanger Geologische Abhandlungen*, **38**: 1–49.
- Sudoł-Procyk, M., Budziszewski, J., Krajcarz, M.T., Jakubczak, M., Szubski, M., 2018. The chocolate flint mines in the Udorka Valley (Częstochowa Upland) – a preliminary report on the field and lidar surveys. In: *Between History and Archaeology Papers in honour of Jacek Lech* (eds. D.H. Werra and M. Woźny): 89–102. *Archaeopress Archaeology*, Oxford.
- Sudoł-Procyk, M., Brandl, M., Krajcarz, M.T., Malak, M., Skrzatek, M., Stefański, D., Trela-Kieferling, E., Werra, D.H., 2021a. Chocolate flint: new perspectives on its deposits, mining, use and distribution by prehistoric communities in Central Europe. *Antiquity*, **95**, e25; <https://doi.org/10.15184/aqy.2021.48>
- Sudoł-Procyk, M., Krajcarz, M.T., Malak, M., Werra, D.H., 2021b. Preliminary characterization of the prehistoric mine of chocolate flint in Poręba Dzierżna, site 24 (Wolbrom commune, Lesser Poland Voivodeship). *Sprawozdania Archeologiczne*, **73**: 109–135; <https://doi.org/10.23858/SA/73.2021.2.2546>

- Sudoł-Procyk, M., Malak, M., Binnebesel, H., Krajcarz, M.T., 2022.** Striped flint in archaeological materials around the outcrops of the Kraków-Częstochowa striped flint variety. *Archaeologia Polona*, **60**: 163–185; <https://doi.org/10.23858/APa60.2022.3099>
- Sulgostowska, Z., 2005.** Kontakty społeczności późnopalolitycznych i mezolitycznych między Odrą, Dźwiną i górnym Dniestrem: studium dystrybucji wytworów ze skał krzemionkowych (in Polish). Instytut Archeologii i Etnologii PAN, Warszawa.
- Šebela, L., Přichystal, A., Škrdl, P., Humpolová, A., 2017.** Unusual Middle Paleolithic stone tool from southern Moravia with possible relations to southern Poland. *Acta Archaeologica Carpathica*, **52**: 289–297.
- Trnka, G., 2004.** Niederbayerischer Hornsteinimport in das niederösterreichische Donautal im Raum Melk. In: *Zwischen Karpaten und Ägäis. Neolithikum und Ältere Bronzezeit* (Gedenkschrift für Viera Němejcová-Pavůková) (eds. B. Hänsel and E. Studeníková): 309–321. *Internationale Archäologie – Studia honoraria* 21.
- Vávra, M., 1993.** Neolitická plastika z Černožic (in Czech). *Archeologické rozhledy*, **45**: 212–220.
- Vencel, S., 1971.** Současný stav poznání postmesolitických štípaných industrií v Československu (in Czech). In: *Z badań nad krzemieniarstwem neolitycznym i eneolitycznym* (ed. J.K. Kozłowski): 74–99. Muzeum Archeologiczne, Kraków.
- Vencel, S., 1978.** Voletiny – nová pozdně paleolitická industrie z Čech (in Czech). *Památky archeologické*, **69**: 1–44.
- Voláková, S., 2001.** K technologii štípané industrie magdalénien: analýza jader z jeskyně Pekárny (in Czech). *Časopis Moravského muzea. Vědy společenské*, **86**: 101–116.
- Weber, K.H., 1978.** Erläuterungen zur Geologischen Karte 1:25000 7137 Abensberg. Bayerisches Geologisches Landesamt, München.
- Weißmüller, W., 1995.** Flintsbach-Hardt and the Jurassic hornstones of the Ortenburger Kieselnirenkalke in SE-Bavaria. *Archaeologia Polona*, **33**: 287–295.
- Wilczyński, J., 2016.** A new beginning: modern humans in Poland. In: *The Past Societies. Polish lands from the first evidence of human presence to the early Middle ages. Volume 1:500,000 – 5,500 BC* (ed. J. Kabaciński): 111–128. Institute of Archaeology and Ethnology Polish Academy of Sciences, Warszawa.
- Zeiss, A., 1964.** Zur Malm Gamma/Delta-Grenze in Franken. *Geologische Blätter für Nordost-Bayern*, **14**: 104–115.
- Zeiss, A., 1977.** Jurassic stratigraphy of Franconia. *Stuttgarter Beiträge zur Naturkunde, Serie B*, **31**: 1–32.
- Zeiss, A., 2012.** Lithostratigraphische Einheiten des Jura in Nordbayern. *Geologische Blätter für Nordost-Bayern*, **62**: 247–260.